PREDICTION OF SURFACE ROUGHNESS IN ADDITIVELY MANUFACTURED SAMPLES

A DISSERTATION

SUBMITTED IN PARTIAL FULFILLMENT OF THE REQUIREMENTS FOR THE

AWARD OF THE DEGREE

OF

MASTER OF TECHNOLOGY

IN

PRODUCTION ENGINEERING

Submitted by

ANUJ SAXENA

(2K21/PRD/12)

Under the supervision of

Prof. QASIM MURTAZA   **Dr. PARAS KUMAR**

(Mechanical Engineering Department)

DEPARTMENT OF MECHANICAL ENGINEERING

DELHI TECHNOLOGICAL UNIVERSITY

(Formerly Delhi College of Engineering)

Bawana Road, Delhi-110042

JUNE, 2023

DELHI TECHNOLOGICAL UNIVERSITY

(Formerly Delhi College of Engineering)
Bawana Road, Delhi-110042

CANDIDATE'S DECLARATION

I, ANUJ SAXENA, Roll No. 2k21/PRD/12 student of M.tech (Production Engineering), hereby declare that the project Dissertation titled "**Prediction of surface roughness in additively manufactured samples**" which is submitted by me to the Department of Mechanical Engineering, Delhi Technological University, Delhi in the partial fulfillment of the requirement for the award of degree of Masters of Technology, is original and not copied from any source without proper citation. This work has not previously formed the basis for the award of any Degree, Diploma Associateship, fellowship or other similar title or recognition.

Place: Delhi   ANUJ SAXENA

Date:

CERTIFICATE

I hereby certify that the Project Dissertation titled "**Prediction of surface roughness in additively manufactured samples**" which is submitted by ANUJ SAXENA 2K21/PRD/12, Mechanical Engineering Department, Delhi Technological University, Delhi in partial fulfilment of the requirement for the award of the degree of Master of Technology, is a record project work carried out by the student under my supervision. To the best of my knowledge this work has not been submitted in part or full for any Degree or Diploma to this University or elsewhere.

Place: Delhi
Date:

Prof. QASIM MURTAZA
(SUPERVISOR)
Department of Mechanical Engineering
Delhi Technological University, Delhi

Dr. PARAS KUMAR
(CO-SUPERVISOR)
Department of Mechanical Engineering
Delhi Technological University, Delhi

ACKNOWLEDGEMENT

ABSTRACT

Artificial intelligence (AI) and additive manufacturing (AM) are excellent and revolutionary technologies. The most recent technology for producing objects through layer-over-layer deposition is called additive manufacturing (AM). Based on the thermal analysis of bonding formation in the 3D printed parts, the mechanism model of surface roughness was established. Most of the printing parameters, including infill density (ID), printing speed (PS), nozzle temperature (NT), and layer height (LH), deposition road width, and printing platform temperature, were considered to ameliorate the surface morphology of printed parts. The main objective of this research work is to predict surface roughness in additively manufactured processes in PLA+ polymer material by using different machine learning algorithms like linear regression, support vector machine (SVM), and two ensemble learning techniques: – Xtreme gradient boosting (XGBoost) and random forest regressor and also characterization of the material . Taguchi's Design of the Experiment was used to make L25 orthogonal array sample datasets, compare all the machine learning algorithms to see which one has the best model-fit accuracy. The machine model works on five key input parameters that influence layer geometries: layer height (LH), infill density (ID), printing speed (PS), and nozzle temperature (NT) with a 0^0 raster angle. By applying all ML algorithms, random forest regression is the best model, which gives 94.85% accurate results in the datasets with a minimum mean squared error of approx. 0.3756 and a maximum r2_score of approx. 0.92154. XRD shows the PLA+ material is semi crystalline material and the peak is about to 18^0 with 2θ.

Keywords: *Additive manufacturing, Polymers, PLA+ material, Machine learning, Fused deposition modeling, XRD.*

TABLE OF CONTENTS

LIST OF ABBREVIATION

ML	Machine learning
AM	Additive manufacturing
3D	Three dimensional
RP	Rapid prototyping
FDM	Fused deposition modelling
PLA	Poly lactic acid
ASTM	American society of testing and materials
AI	Artificial intelligence
FFF	Fused filament fabrication
ABS	Acrylonitrile butadiene styrene
PLA+	Poly lactic acid+
MSE	Mean squared error
RMSE	Root mean square error
Ra	Surface roughness
PS	Printing speed
ID	Infill density
LH	Layer height
PS	Printing speed
XRD	X-ray diffraction
LOM	Laminated object manufacturing
CAD	Computer aided design
CAM	Computer aided manufacturing
CNC	Computer numerical controlled

LIST OF FIGURES

LIST OF TABLES

CHAPTER 1

INTRODUCTION

1.1.BACKGROUND AND MOTIVATION

Machine learning (ML) is a subgroup of artificial intelligence (AI) that has gained popularity in the field of additive manufacturing (AM) industrial research. AM, also referred to as 3D printing or rapid prototyping (RP), involves the creation of objects by layering materials on top of each other, controlled by a computer-aided design model. Machine learning, on the other hand, refers to computer programming techniques used to optimize performance based on experimental data or past experiences.

In the context of additive manufacturing, machine learning goes beyond the conventional application of making predictions through data setup. The industrial research community is actively investigate innovative ideas to incorporate machine learning into AM processes. By leveraging machine learning techniques, researchers aim to enhance various aspects of additive manufacturing, such as improving print quality, optimizing process parameters, and enabling automated decision-making. AM is an advanced manufacturing technology that creates three-dimensional objects by joining materials together in a layer-by-layer manner. It relies on a computer-aided design (CAD) model to guide the fabrication process. This technology has gained significant attention due to its ability to produce complex geometries, customized designs, and rapid prototyping capabilities. By combining machine learning with additive manufacturing, researchers seek to unlock new possibilities and further enhance the capabilities and efficiency of this manufacturing technique [1].

The current state of additive manufacturing (AM) faces a significant challenge regarding the inconsistent quality of 3-D printed products, which heavily relies on various processing parameters like layer thickness and printing speed. To tackle this challenge, two approaches are commonly employed: conducting experiments or utilizing high-fidelity simulations. However, both methods can be time-consuming, expensive [2]. Another approach to confirm sample quality and process reliability is the implementation of in situ monitoring systems. Nonetheless, an effective and efficient tool is needed for

error and defect detection using in situ data, like as images [3]. In both experimental and in situ monitoring approaches, there is a crucial need for a systematic tool for mining and data analysis. This requirement is being addressed by machine learning (ML). ML models learn from reliable training datasets and acquire knowledge that they utilize for making inferences and predictions. This capability enables trained ML models to efficiently determine optimal processing parameters and make predictions. Recent literature also reports various ML applications, including geometric deviation control, cost estimation, and quality assessment. The utilization of ML in these applications demonstrates its role as a vital component of Industry 4.0, as it empowers effective data manipulation and analysis. In [4] one of the most commonly utilized AM processes is FFF, which falls under the category of material extrusion. FFF involves the fabrication of objects by feeding a continuous filament of thermoplastic material into an extruder head. The filament is heated within the extruder head and then deposited onto a base build plate, allowing for the layer-by-layer construction of the desired object. In [5] Recent studies have suggested that the application of machine learning techniques holds the potential to enhance predictive performance and increase productivity in the industrial sector. AM is a promising technology for the production of components with intricate geometries. It offers advantages such as reduced costs, shorter lead times, and the ability to manufacture intricate parts without the demand for specialized tools as opposed to traditional manufacturing methods [6].

1.2. ADDITIVE MANUFACTURING

Additive manufacturing, as a process, originated in the mid-1980s with the commercialization of an advanced version of stereolithography (SL). Over the years, additional techniques such as laminated object manufacturing, fused deposition modeling, and 3D printing have also been commercialized. The industrial applications of additive manufacturing parts have demonstrated its widespread recognition as a technology that addresses various challenges across diverse industries. Despite its advantages, the high cost of additive manufacturing machines makes them inaccessible to medium and small enterprises. To overcome this limitation, the implementation of web-based additive manufacturing systems can significantly enhance the productivity, manufacturing speed, and economic advantages for such firms [7]. By providing online access to additive manufacturing capabilities, these systems enable smaller enterprises to

leverage the benefits of the technology without the need for significant investments in expensive equipment. Traditionally, the manufacturing of three-dimensional (3D) solid parts concern the removal or shaping of material from a workpiece block to achieve the desired shape, using computer-aided design (CAD) files from software like SolidWorks, CATIA, Pro-E, UG, and AutoCAD. However, conventional machining processes have limitations when it comes to manufacturing complex components. In the case of molding processes, the cost of molds is typically high, and their accuracy decreases after producing batches of parts. Thermal molding techniques, such as injection molding, also require expensive molds and are more economically viable for large production runs that demand reproducibility. To streamline these manufacturing operations, computer-aided manufacturing (CAM) processes can be utilized, which enable automation. However, these processes are costly and time-consuming, often requiring repetitive iterations to achieve the desired final manufacturing outcome for a part, model, or prototype [8]. Therefore, there is a clear requirement for a straightforward and efficient process and apparatus that allows designers to design and fabricate 3D objects at their office workstations with the same ease and clarity as using a printer and desktop computer. This should be accomplished in a cost-effective manner. With the development of desktop computers and subsequent advancements in CAM, CAD, and CNC, coupled with the growth and accessibility of materials and automotive industrial lasers, a new paradigm known as rapid prototyping (RP) has emerged to address the aforementioned need. Rapid prototyping (RP) is a broad term encompassing various technologies that enable the direct manufacture of physical product from computer-aided design data sources [9]. In RP, object is constructed by depositing layers in a two-dimensional plane (x-y). The third dimension (z) is achieved by stacking these layers on top of each other, although the z-coordinate is not continuous [10]. Additive manufacturing methods share a common characteristic of building 3D objects by joining materials layer by layer, which stands in contrast to classical methods like milling and forging. While additive manufacturing involves the addition of material, classical methods involve removing material or applying mechanical forces to permanently deform it into the desired shape. Although the overall fabrication process is similar across different additive manufacturing methods, the specific system determines the mechanism by which different layers are created and bonded. Figure 1.1 illustrates the fundamental steps involved in the RP process.
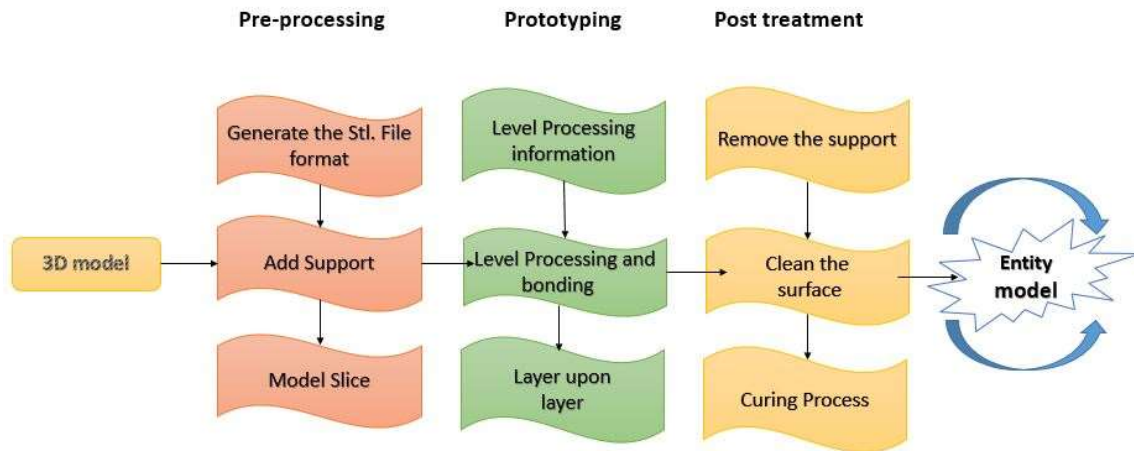
Figure 1.1: Step by step procedure in Rapid Prototyping process

The initial step in the additive manufacturing process involves creating a model using any solid modeling software. A suitable solid geometry is chosen to generate data that will effectively control the fabrication process. Typically, the part manufactured procedure is divided into two distinct steps.

Step 1: During this stage, the CAD file is saved in .stl format and then being converted into a triangular meshing. The sliced triangular meshed file is then stored in standard file formats that can be interpreted by the additive manufacturing machines in the subsequent phase. Parameters such as layer thickness and part orientation play a crucial role in minimizing costs and build time.

Step 2: This step varies across different additive manufacturing processes and depends on the specific fabrication mechanism of the respective machine. The machine's dedicated software guides the laser path or instructs the extrusion head, utilizing the instruction obtained from step 1. Additionally, process-related details such as allowances, tolerances, material specifications, and machining types are obtained to the machine's controller [11].

Additive manufacturing techniques can be broadly classified into five main categories: Selective Laser Sintering (SLS), Fused Deposition Modeling (FDM, Stereolithography (SL), Binder Jet and Laminated Object Manufacturing (LOM). Fused Deposition Modeling, (FDM), which belongs to the material extrusion process category, is widely recognized and employed in additive manufacturing. FDM manufactured objects by

using a layer by layer deposition of filament of thermoplastic material, which is heated in an extruder head and then stick onto a build plate [12].

1.2.1. Stereolithography(SL)

Stereolithography was orginate by scientist Chuck Hull in year 1986 and also it was the first commercially available 3D printing technique. SL is an additive manufacturing technique that belongs to the category of vat photopolymerization. It was one of the first additive manufacturing processes to be orginate and commercialized. In SL, a liquid photopolymer resin is exposed to a specific pattern of ultraviolet (UV) light using a laser or other light source. The UV light causes the resin to solidify and form a layer of the desired object. The build platform is then lowered, and a new layer of liquid resin is fall over the previously solidified layer. This process is repeated layer by layer until the entire object is formed. Figure 1.2 illustrates the process of stereolithographic [13]. SL offers high precision and accuracy, making it suitable for producing intricate and complex geometries with smooth surface finishes. The ability to create parts with fine details makes SL popular in applications such as prototyping, product development, and rapid tooling. After the SL process is complete, the part may require post-processing, such as cleaning, curing, and surface finishing, to attain the desired final appearance and mechanical properties.
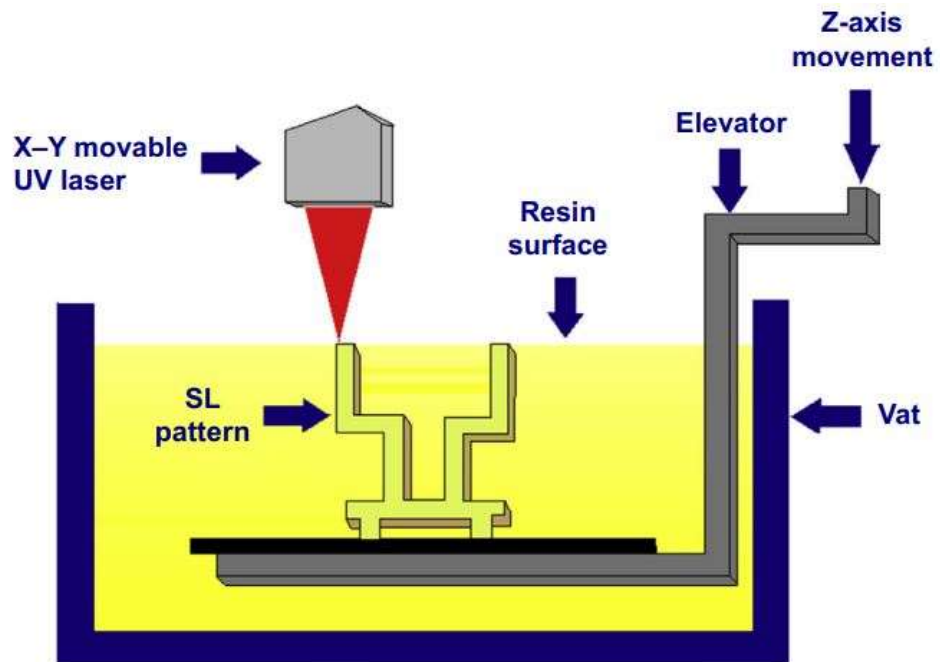
Figure 1.2: Stereolithography 3D printing [13]

Stereolithography finds its application in various fields, including the creation of prototypes for products in the development stage, medical models, computer hardware, and numerous other applications. It offers a fast and versatile solution, capable of producing designs of nearly any complexity. However, it is important to note that stereolithography can be relatively expensive [14].

1.2.2. Laminated Object Manufacturing (LOM)

The process involves placing a layer of material, coated with adherent on one side, onto a build platform with the sticking side facing down. A heated roller is then passed over the material, ensuring it adhesive to the platform securely. Next, laser beam follows profile of a specific slice of the desired part, cutting through the layer of material. The lasered beam also crosshatches the areas that do not form part of the current cross-section, cutting through the material again.

After completing the slice, the platform is lowered by the thickness of one layer, and another layer of material is affixed on top of the previous layer. The procedure is then repeated for the next cross-section slice of the part. This layer-by-layer process continues until all the cross-section slices have been added. Once the entire part has been formed, it is removed as a solid block from the platform. The crosshatched areas within the block are subsequently broken away from the finished part, leaving behind the desired object. For a visual representation of this process, please refer to Figure 1.3 [15].
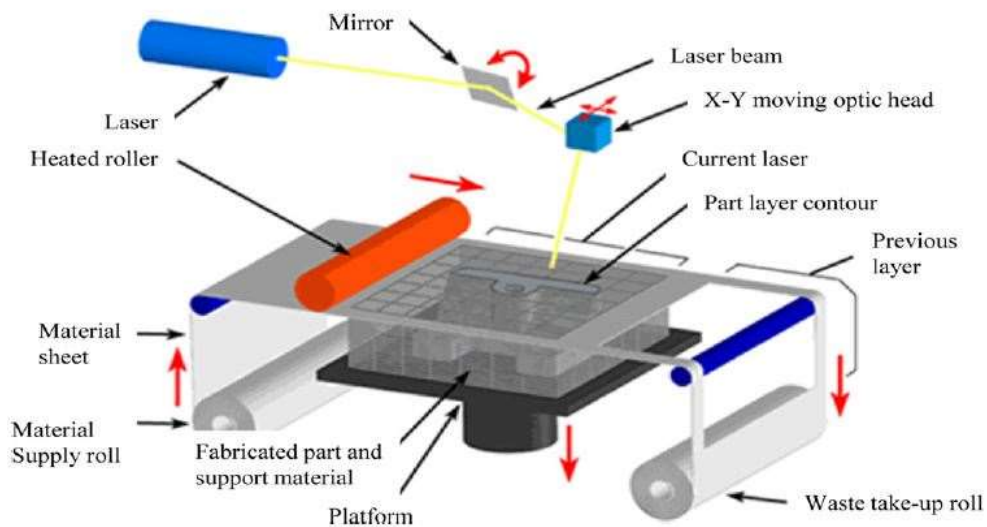
Figure 1.3: Laminated object manufacturing [15]

LOM combines both additive and subtractive manufacturing methods. The process begins by adhering a sheet of paper or artificial/synthetic polymer to a subtract using a laminated roller. When once the layer is in place on the building platform, a CO_2 laser or blades joined to the print head follow the outline path of the layer based on the computer aided design file. The platform then goes down, allowing for a new sheet of building material to be added. This cutting process is repeated layer over layer. LOM offers a rapid solution for printing objects with greater dimensions and higher build speeds compared to other AM techniques. However, it's important to note that the material used within a given coat must be consistent. Since the build material remains fixed within the model contour during the lamination process, there is no need for a support material [16].

1.2.3. Selective Laser Sintering (SLS)

SLS is an AM process that utilizes a powerful laser beam, such as CO2 or Nd: YAG, to soften, melt, and solidify a powder material. The process involves the following steps: A thin layer of powder material, which can be wood, acrylic, plastic, metal, protein, ceramic, or other suitable materials, is evenly spread onto a build stage using a roller. The powerful laser beam is then directed onto the powder layer, selectively fusing and solidifying the particles based on the cross-sectional design of the model. The laser focuses only on specific areas, allowing for precise control over the sintering process. Once a layer is complete, the build platform moves downward, and this process repeats layer over layer. Each subsequent layer is fused to the previous one, gradually building the desired object [16].

One advantage of SLS is that the unsintered powder material surrounding the printed object can serve as support material. This not only reduces the need for additional support structures but also allows for the reuse or recycling of unused powder, minimizing material waste. Please refer to Figure 1.4 for a visual representation of the process. The surface roughness of the printed object are influenced by the size of the powder particles. Larger particle sizes result in higher roughness and lower spatial resolution, as they affect the level of detail and smoothness achievable in the final printed object [17]. SLS demonstrates its true excellence in the production of long-lasting plastic components. SLS parts are renowned for their strength and can match the quality of parts manufactured through conventional methods such as injection molding. SLS finds extensive application

in various industries, including automotive and aerospace, where it is utilized to create durable end use products.
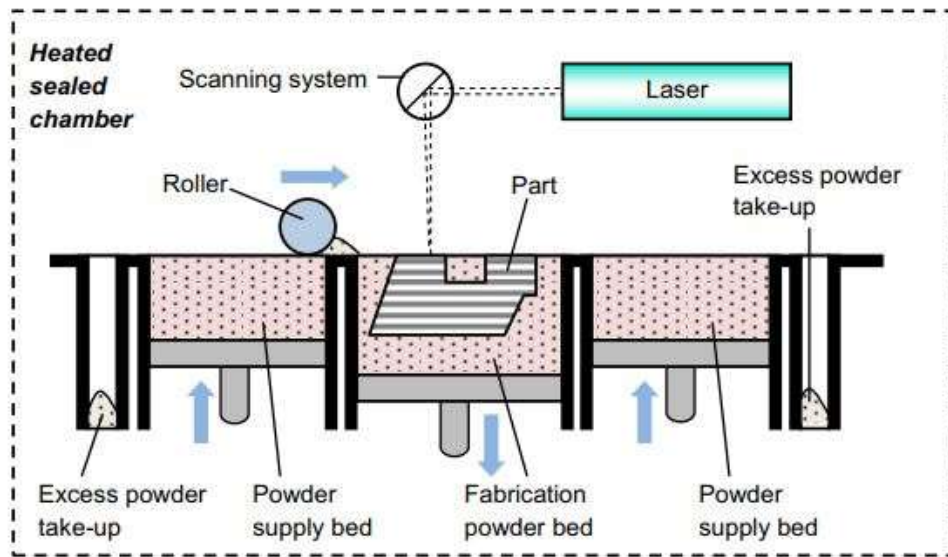
Figure 1.4: Selective laser sintering [18]

1.2.4. Binder jet additive manufacturing(BJAM)

BJAM is a process that involves the selective jetting of a fluid binder onto consecutive layers of powder material, typically at near-room temperature. This process enables the production of complex geometries according to the design specifications. The resulting parts, known as green parts, may require additional steps such as sintering and debinding to achieve the best dimensional accuracy, density, and mechanical properties [19].

During the BJAM process, the powder bed serves as active support for the deposited binder. It ensures the stability of the printed structure and allows for the layer-by-layer construction. Importantly, there is no any type of direct physical contact between the jetting assembly and the deposited powder, as demonstrated in Figure 1.5. After the binder is applied to each layer, the green parts can undergo subsequent treatments, such as debinding, where the excess binder is removed from the printed object, and sintering, a high-temperature process that fuses the powder particles together to enhance their strength and durability. These post-processing steps are crucial for achieving the desired final dimensional accuracy, density, and mechanical properties of the printed parts [20].
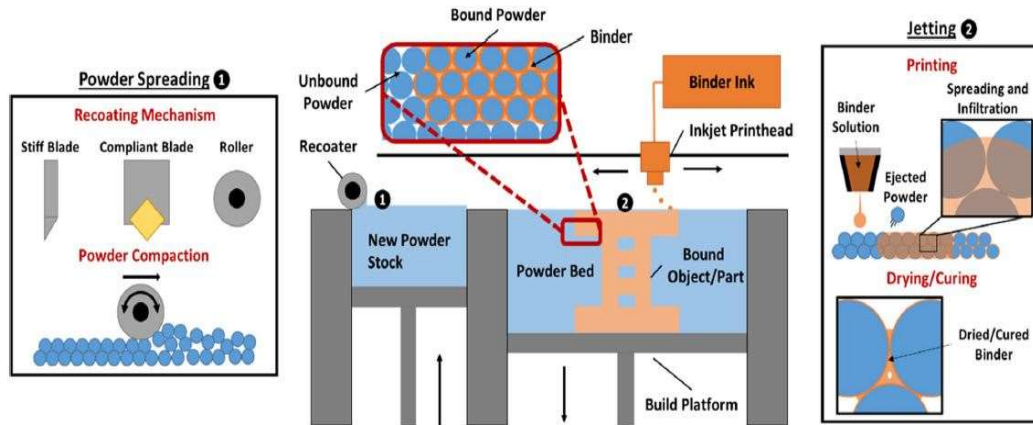
Figure 1.5: Detailed image of BJAM
(1) Powder spreading variations and (2) powder-binder interactions during jetting [19]

1.2.5. Fused Deposition Modelling

FDM is a widely used and environmentally friendly AM process for creating highly intricate products in both domestic and industrial sectors. It operates by extruding a thin filament of molten material, typically a thermoplastic, through a heated nozzle [21]. This nozzle is attached to a movable arm that can traverse the X, Y, and Z axes according to the specifications of the 3D model. The FDM process start with a solid 3D model created using computer aided design software. The model is sliced into thin layers, and the FDM machine starts building the object layer by layer. The heated nozzle deposits the molten material onto the build platform, where it solidifies upon cooling and fuses with the previous layer. This layer-over-layer deposition continues until the whole object is formed. The components of FDM machines are designed to work together seamlessly, enabling efficient and precise part fabrication while minimizing material waste and the need for additional tooling. Figure 1.6 illustrates the integration of various components in FDM machines to facilitate the rapid and cost-effective production of parts.

Fused Deposition Modeling (FDM) has become a popular choice for additive manufacturing due to its versatility, accuracy, and ability to produce complex geometries. It offers a practical and accessible solution for creating 3D printed objects, both for personal and industrial applications.
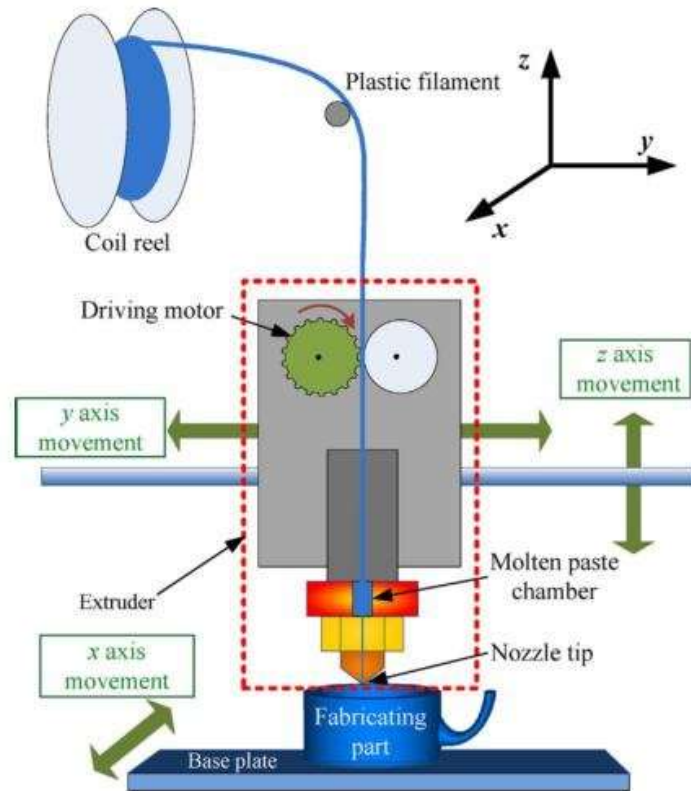
Figure 1.6: Schematic of detailed image of FDM [22]

The FDM (Fused Deposition Modeling) process begins with the design and development of the desired model using CAD software. The CAD file is then converted into a readable format known as standard triangle language (STL) using specialized software packages that are compatible with FDM 3D printers.

During printing, the FDM printer utilizes stepper motors to feed and push a solid filament of material through a nozzle [21]. The filament is melted at a specific temperature by the extruder and then deposited onto the building platform. The molten material rapidly solidifies and adheres to the platform to form each layer of the object. This layer-by-layer process is guided by numerical G-codes, which instruct the printer to repeat the deposition procedure until the complete object is formed. While a different range of materials, including low-temperature metal alloys and composites, can be used in FDM, thermoplastics and polymer-based composites are the primary materials employed. The quality of the printed product and its mechanical properties depend on various factors, such as the orientation of the build, nozzle temperature, infill density, infill pattern, nozzle diameter, layer thickness and printing speed [23].

It is crucial to optimize these parameters to achieve a satisfactory product with desirable mechanical properties. Suboptimal conditions or inadequate temperature control can result in printing issues like warpage and shrinkage, which can affect the overall quality and accuracy of the printed object.

1.3. MACHINE LEARNING

ML, a component of AI, encompasses the creation of algorithms and statistical models that empower computers to acquire knowledge from data without explicit programming. Put simply, machine learning entails training computers to identify patterns within data, allowing them to generate predictions or decisions based on the information at hand [24]. Machine learning algorithms find utility across a broad spectrum of applications, spanning from speech recognition and image to fraud detection and recommendation systems. The ML process generally encompasses several stages, which include data preprocessing, model training, and model evaluation [25]. Throughout the training phase, the algorithm is exposed to an extensive dataset and adapts its internal parameters to identify patterns within the data. The model's effectiveness is subsequently assessed using a distinct dataset, and the algorithm is iteratively refined until it attains an acceptable level of accuracy. Various types of machine learning algorithms exist, as listed below [26].

1. Supervised learning
2. Unsupervised learning
3. Reinforcement learning

1.3.1. Supervised Learning

Supervised machine learning is a branch of ML where an algorithm learns to make predictions or decisions based on labeled training data. In this type of learning, the algorithm is provided with a dataset in which each example consists of input features and their corresponding known outputs or labels. The algorithm analyzes this labeled data to identify patterns, relationships, or statistical dependencies between the input variables and the output variables. It uses this information to create a model that can generalize its learning and make accurate predictions or decisions on new, unseen data. The main goal of supervised machine learning is to teach the algorithm to map inputs to outputs, allowing it to make reliable predictions on new, unlabeled data.

Supervised learning is highly versatile and applicable to various tasks, including classification and regression. In classification tasks, the algorithm acquires the capability to categorize inputs into distinct classes or categories. For instance, it can be trained to discern whether an image depicts a cat or a dog. In regression tasks, the algorithm learns to forecast a numerical value based on the given input. For instance, it can be train to estimate the price of house based on factors like its location and size. Supervised learning thus enables algorithms to discern patterns and make informed decisions or predictions across a wide range of problem domains [27].

1.3.2. Unsupervised learning

Unsupervised machine learning involves an algorithm learning to uncover patterns in data without relying on labeled data or explicit feedback. In unsupervised learning, the algorithm works with an unlabeled dataset and seeks to identify inherent patterns, structures, or relationships within the data. The primary objective of unsupervised learning is typically to unveil hidden relationships, groupings, or anomalies present in the data. Unsupervised learning proves valuable for various tasks including anomaly detection, clustering, and dimensionality reduction. In clustering tasks, the algorithm group's similar data points together, forming distinct clusters. For instance, it can be utilized to group customers based on their purchasing behaviors. In dimensionality reduction tasks, the algorithm reduces the number of variables or features in the data while retaining as much relevant information as possible. For example, it can be employed to decrease the dimensionality of an image dataset. In anomaly detection tasks, the algorithm identifies data points that significantly deviate from the rest of the data. For instance, it can be used to detect instances of credit card fraud. Overall, unsupervised learning enables algorithms to discover valuable insights and patterns in data without relying on predefined labels or feedback [27] - [28].

1.3.3. Reinforcement learning

Reinforcement learning is a ML paradigm wherein an agent learns to make optimal decisions through feedback from its environment. In this learning approach, the agent actively engages with an environment and receives rewards or penalties based on its actions. The ultimate objective for the agent is to acquire a policy, which is essentially a mapping from states to actions that maximizes the cumulative reward over time.

Reinforcement learning finds wide application in diverse domains, including robotics, game playing, and control systems. For instance, a reinforcement learning algorithm can be employed to train a robot to navigate a maze or to teach an agent how to proficiently play games such as chess or go. By iteratively exploring the environment and optimizing its decision-making process, the agent gradually improves its performance and attains proficiency in complex tasks. The process of reinforcement learning typically involves several steps, including defining the state and action spaces, defining the reward function, and selecting an appropriate algorithm for learning the policy. The agent learns by exploring the environment and updating its policy based on the rewards it receives [27]–[29]

1.4. SURFACE ROUGHNESS

Surface roughness in Fused Deposition Modeling (FDM) refers to the irregularities or rough texture observed on the outer surface of a 3D printed object. It is a measure of the deviation of the surface profile from its ideal or smooth form. Surface roughness is typically quantified using parameters such as Ra (arithmetical mean roughness) or Rz (maximum peak-to-valley height). The layer height, which determines the thickness of each printed layer, has a direct impact on surface roughness. Smaller layer heights result in finer steps between layers, leading to smoother surfaces [30] it is calculated by microns. Surface roughness is commonly characterized using three key parameters: Ra, Rz, and Ry. These parameters provide insights into different aspects of the surface irregularities and their values are determined as follows:

Arithmetical Mean Deviation of the Profile (Ra): Ra represents the average deviation of the profile from the mean line (see in figure 1.7). It is calculated by measuring the absolute values of the surface deviations from the mean line within a specified sampling length, L, and then computing their arithmetic mean.

Point Height of Irregularities (Rz): Rz measures the maximum height of irregularities on the surface. It is determined by evaluating the average of the five largest peak heights and the average of the five largest valley depths within the sampling length. Rz provides information about the height variations of the surface.

Maximum Height of the Profile (Ry): Ry indicates the maximum height between peak contour lines and the contour line from the bottom. It represents the overall depth or height of the surface irregularities within the sampling length, L.
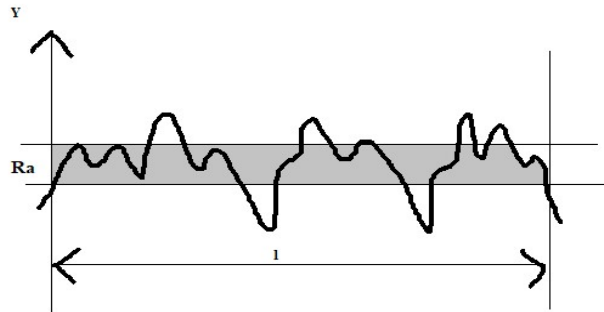
Figure 1.7: Surface roughness 3d FDM sample Ra (µm) [30]

$$Ra = \frac{1}{n}\sum_{i=1}^{n} y_i \qquad\qquad\qquad \text{Eq. 1.}$$

Material Selection: Different filament materials have varying characteristics that can impact surface roughness. Some materials inherently exhibit smoother surfaces than others. Experimenting with different materials and selecting those with smoother surface finishes can help improve the final print's surface quality. Proper cooling during the printing process can help reduce surface roughness. Sufficient cooling time between layers allows the filament to solidify more effectively, minimizing sagging or warping. Adjusting fan settings and utilizing cooling mechanisms on the printer can aid in achieving smoother surfaces.

To optimize surface roughness in FDM, it is advisable to experiment with different print settings, including layer height, nozzle diameter, print speed, and cooling parameters. Additionally, employing post-processing techniques tailored to the specific requirements of the print can further refine the surface quality. To assess the surface roughness of additive manufacturing (AM) parts, the usual method involves using a profilometer and Taylor Hobson equipment to calculate the arithmetical mean height of a line, known as Ra. However, it's important to note that the surface structure of AM parts is influenced by factors such as the overlap of hatches and the chosen hatch strategy.

1.5. THE APPLICATION OF 3D PRINTING IN INDUSTRIAL SECTOR

Just like any other manufacturing process, 3D printing requires the use of high-quality materials that adhere to consistent specifications in order to create consistent and high-

quality devices. To ensure this, protocols, standards, and agreements regarding material controls are established between purchasers, suppliers, and end-users of the materials. 3D printing manufacturing has the capability to produce fully functional parts using a diverse array of different materials, including metals, ceramics, polymers, as well as their combinations in the form of composites, hybrids, or functionally materials [31].

1.5.1. Aerospace industry

Figure 1.8: Turbine with hub casing [32]

3D printing technology offers unparalleled design freedom and production capabilities in the manufacturing of components. Particularly in the aerospace industry, 3D printing has the ability to create lightweight parts with improve and intricate geometries, leading to reduced energy consumption and resource utilization [33]. Additionally, the use of 3D printing can result in fuel savings as it minimizes the amount of material required for aerospace parts production. Furthermore, 3D printing has found extensive application in the production of spare parts for aerospace components like engines (see in figure 1.8). Given the susceptibility of engine parts to damage and the need for regular replacements, 3D printing technology presents an effective solution for procuring such spare parts [34]. In the aerospace industry, nickel-based alloys are highly preferred due to their desirable tensile properties and resistance to corrosion, and ability to withstand damage.

1.5.2. Automotive industry

Figure 1.9: Knuckle joint [35]

In recent times, the advent of 3D printing technology has brought about rapid transformations in various industries, enabling them to revolutionize their approaches to design, development, and manufacturing. In the automotive industry specifically, the utilization of 3D printing techniques has ushered in remarkable advance, leading to the creation of lighter and more intricate structures within shorter timeframes (refer in figure 1.9). Ford has emerged as a leader in employing 3D printing technology, utilizing it to produce prototypes and engine parts [36]. BMW leverages 3D printing technology to manufacture hand-tools for automotive testing and assembly, while AUDI collaborated with SLM Solution Group AG in 2017 to produce spare parts and prototypes [37].

1.5.3. Healthcare and Medical Industry

3D printing technology has the capability to fabricate cartilage and bone structures that can be used to replace voids resulting from trauma or disease [38]. It also holds potential for the replacement, restoration, maintenance, or improvement of tissue functionality. Tissues generated through 3D printing exhibit joins pore networks, biocompatibility, appropriate surface chemistry, and favorable mechanical properties [39].
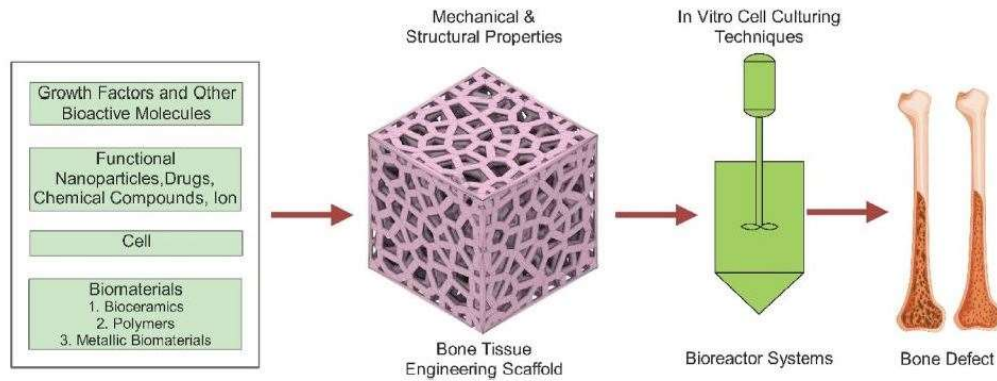
Figure 1.10: Bone tissue engineering strategy [40]

Moreover, 3D printing can be utilized to produce models simulating organ failures caused by critical conditions such as diseases, accidents, or birth defects (refer in figure 1.10). These 3D-printed models can serve as valuable tools for neurosurgeons to practice surgical techniques, improving accuracy, reducing training time, and offering hands-on training opportunities that simulate real patient conditions.

1.5.4. Architecture, building, and construction industry

Figure 1.11: 3d printed site model [41]

3D printing technology offers significant environmental benefits and enables the realization of highly complex geometries. In the construction industry, it has the potential to revolutionize the way buildings are created by allowing the printing of entire structures

or construction components (refer in figure 1.11). The integration of Building Information Modelling (BIM) further enhances the utilization of 3D printing technology. BIM provides a digital representation of a building's functional and physical characteristics, enabling the sharing of information and knowledge throughout its life cycle, from initial conception to demolition. This comprehensive and collaborative technology serves as a reliable source for decision-making during all stages of construction and design [42]. By leveraging 3D printing technology, companies can swiftly and cost-effectively design and visualize buildings, thereby avoiding delays and identifying potential problem areas. Moreover, it facilitates improved communication and understanding between construction engineers and their clients. Rather than relying on traditional methods like paper and pencil, 3D printing simplifies the process of transforming customer ideas into tangible representations [43].

1.5.5. Electronic and electric industry

Figure 1.12: 3d printing in electronic industry [44]

The utilization of Fused Deposition Modeling in the 3D printing technique for the production of 3D electrodes offers a cost-effective and time-efficient approach for mass production of electrode materials. When compared to commercial electrodes like aluminum, copper, and carbon, the design and surface area of the 3D electrode can be

easily tailored to specific applications (refer in figure 1.12). Additionally, the 3D printing process for these electrodes is fully automated and provides a high level of precision, enabling the completion of printing for eight electrodes in just 30 minutes. There is a pressing need in today's society for the development of environmentally friendly electronic devices that possess low manufacturing costs, ensure safety, exhibit high reliability, and allow for rapid production. This highlights the significance and demand for the production of such devices [45].

CHAPTER 2.

LITERATURE REVIEW

According to recent studies, the implementation of ML methods may provide both improved speculate performance and increased productivity in the industrial sector. AM is an auspicious technology to manufactured samples with intricate geometries. It can fabricate complex parts with minimum price and take time and without using special tool system like molds compared to traditional manufacturing technologies.

D. Horvath et al [9], the DoE method was used to examine the impact of machine parameters on printed component surface roughness. The impact of model temperature, layer thickness, and part fill style on the surface roughness of FDM-built parts was studied that all factors were found to have a significant effect on surface roughness, with layer thickness having the greatest impact. Reducing the layer thickness resulted in decreased roughness.

Wang et al. [23] discussed that due to the various types of 3D printers, materials, and slicing software available, experimental methods may not be able to produce consistent results that accurately reflect the material's behavior in reality. Additive manufacturing, also referred to as AM, is the method of joining the material (layer-by-layer deposition) with the help of 3D models. In comparison with subtractive manufacturing techniques, AM is defined by the ASTM as "a process of incorporating materials to create 3D objects from 3D model data, generally layer upon layer deposition [46].

FDM is "a material extrusion process that is used to make polymer material parts by the heating of material filaments and the deposition of material layer by layer and make 3d objects"[47].The roughness of a surface plays a significant role in machining processes because it has a direct impact on the functional specifications of the machined parts [48]. According to a survey, FDM is the most frequently utilized AM technology at the present time. One of the main areas of focus for enhancing FDM part quality has been the development of predictive models that link process factors and material qualities with the printed part properties [49]. The investigation detailed in reference number [50] demonstrates how different machine configurations affect surface roughness. It was discovered that the height of the slice and the width of the raster have an impact on surface roughness.

Meanwhile, P.K. Rao et al. [51] conducted experiments to determine the machine settings that result in the smoothest surface finish, which is associated with high temperatures, thin layers, and a high feed/flow rate ratio.

Similarly, R. Anitha et al. [52] reports on similar research where the thickness of the deposited filament, layer height, and extrusion speed were found to affect surface roughness. To address this issue, theoretical modeling and finite element analysis were used to connect the mechanical properties of 3D-printed samples with material and process parameters [53]. However, the complex microstructure of 3D-printed parts, such as irregular pores and surface interactions, make it difficult to accurately model and simulate. Therefore, the accuracy and reliability of these methods are uncertain. To overcome these challenges, ML techniques, as a form of AI, can learn patterns between input features and output results automatically based on training data, without explicit programming [54]. In the context of the AM process, the use of ML may provide effective solutions to the aforementioned issues [55]. The quality of parts produced by FFF can be impacted by variations in the thermal influence between layers during the layer-by-layer material deposition process. Such variations can cause issues like surface roughness, microstructural defects, and poor mechanical properties.

To address this, Boschetto et al. [56] developed a predictive modeling strategy to evaluate the surface roughness of Fused Filament Fabrication-printed items, and this strategy was illustrate through a series of investigation.

Boschetto and Bottini [57] also developed a model that can predict surface roughness of FFF-printed parts that underwent barrel finishing. Reeves and Cobb [58] created an analytical model that examined the effects of surface angle, layer thickness, layer composition and layer profile angle on the surface roughness of stereolithography-printed parts.

Ahn et al.[59] developed a technique for predicting the surface roughness of samples using geometric data from an STL file. They fabricated different specimens on an SLA 3500 machine and measured their surface roughness with a profilometer.

Mishra and colleagues [60], [61] conducted experiments to examine how six different process parameters affect the mechanical strength of samples manufactured by FDM). The parameters included layer thickness, part orientation, raster angle, air gap, raster width and contour number. The significance of each process parameter was determined using an analysis of variance. The study's findings revealed that air gap, contour number, and part orientation had the most substantial impact on the parts' strength.

Pandey et al. [62] introduced a semi-empirical model that aims to forecast the surface roughness of parts produced through Fused Deposition Modeling (FDM). Their study involved conducting experiments where they considered two important process variables: layer thickness and build orientation. By analyzing these variables, the researchers aimed to understand their impact on the resulting surface roughness of the printed parts.

Daekeon et al. [63] presented a theoretical model that aims to explain surface roughness variations based on changes in surface angles and measured data. They successfully utilized interpolation techniques to predict surface roughness. This model provides a framework for understanding the relationship between surface angles and resulting surface roughness, offering insights into the factors influencing the quality of printed parts.

Bellehumeur et al. [64], thermal analysis of the FDM process was conducted. The analysis focused on the heat transfer dynamics of the deposition filament with an elliptical cross-section shape. By studying the thermal behavior during the FDM process, the researchers gained a deeper understanding of the heat distribution and its impact on the final printed part. This thermal analysis contributes to improving the control and optimization of the FDM process parameters, ultimately enhancing the overall quality and performance of the printed parts.

Bharat and colleagues [65] examined how various process parameters, such as air gap, build orientation, layer thickness, road width, and model temperature, affect the surface finish of FDM-built parts. The study employed a fractional factorial design with two levels for each factor. The results indicated that part orientation and layer height had the main impact on surface quality, with a part orientation of 70° and layer thickness of 0.007" yielding the best surface finish. Model temperature, air gap, and road width had minimal effect on the surface finish of FDM parts.

In a similar study, Garg et al. [65] investigated the effects of part orientation on the dimensional accuracy and surface finish of FDM ABS P430 parts at seven different angles (0°, 15°, 30°, 45°, 60°, 75°, and 90° about the Y-axis). They found that part orientation had a considerable influence on both dimensional accuracy and surface finish, with the most desirable outcomes obtained at a 45° angle.

Peârez et al. [66] also investigated surface roughness and dimensional accuracy in ABS P400 parts, creating four prototypes with different slope variations. Past studies have primarily concentrated on creating different methods for estimating surface roughness.

Despite the growing popularity of additive manufacturing (AM), there has been little investigation into using a combination of different sensors and data-driven techniques to predict surface roughness. To address this gap in research, a novel data-driven predictive modeling technique has been developed using machine learning to predict the surface roughness of AM components specifically through the Fused Filament Fabrication (FFF) process.

Scime & Beuth [67] carried out an extensive research investigation focused on defect detection in the laser powder bed fusion (LPBF) process. Their study involved exploring the application of various machine learning and deep learning methods for this purpose. By utilizing these advanced techniques, the researchers aimed to develop effective strategies for identifying and detecting defects in LPBF-printed parts.

Harris at el in [68], [69] describe the predicting process parameters, machine learning techniques can help to circumvent the above-mentioned constraints for FEM. Although large volumes of data are typically needed for these strategies to be more accurate and generalizable. Combining FEM with machine learning can provide you the opportunity to simulate a process (using FEM), forecast or optimise process parameters to achieve desired mechanical qualities. On the one hand, finite element modeling (FEM) is in most cases used for numerical solutions of mathematical models and parameters' optimization, but this process requires deep knowledge on physical properties of material and in-depth understanding of AM process.

Table 2.1: Literature review based on the material.

S.NO.	Author	Material	Process Parameters	Prominent result
1.	Saty Dev, Rajeev Srivastav[12]	ABS (Acrylonitrile Butadiene Styrene)	FDM Process, 1. Layer thickness, 2. Infill pattern, 3. build Orientation	Gyroid pattern, 80% infill,, and 45^0 build orientation gives highest compressive strength all selected parameter of different variable.
2.	Qi feng, Walther, Hans Christian Maier,[70]	PEEK (Poly-Ether-ether-Ketone)	FDM Process, 1. Extruder Temperature 2. Bed Temperature 3. Printing Speed 4. Infill Rate	1. Parameter optimization reducing the residual stress and minimize the warpage effect by the use of Machine learning. XGBoost model predicted that max. stress was 86.7
3.	N. Ahmed, R.K. Abu Al-Rub, I. Barsoum. [71]	Stainless steel 316L	LPBF Process, 1. Laser power, 2. Scanning speed, 3. Hatching spacing, 4. Layer thickness	Primary process parameters including laser power, scanning speed, hatch spacing, layer thickness, give the ideal energy and achieve the highest build density
4.	Raj K. Ohdar,, Siba S. Mahapatra Anoop K. Sood, [72]	ABSP400	FDM Process, 1. Layer thickness, 2. Part build orientation, 3. Raster angle, 4. Raster width. 5. Air gap	1. The reason of low strength is also due to anisotropy, create by the polymer molecules. 2. Optimization is done by ANN gives the max, compressive stress of 17.4751 MPa
5.	Zhengkai Wu, Xin Peng, Hongyixi Bao, Shengchuan Wu, Guozheng Kang,*, [73]	Ti-6Al-4 V	SLM Process, 1. porosity and 2. LOF defects, 3. No. of defects 4. size of defect 5. location, and morphology	1. Use SVM and KNN machine learning algorithm and predict the fatigue life 2. SVM gives best accuracy between predicted and experimental results approximate 0.99.

6.	Rishi Kumar, Rishi Ghosh, Kuldip Singh Sangwan[74]	PLA, ABS , PETG	FDM Process 1. Preheating 2. Printing 3. Standby	PETG is good characterization of all the three material
7.	Ribin Varghese Pazhamannil, P. Govindan, P. Sooraj[75]	PLA	FDM Process 1. Layer thickness (mm) 2. Infill speed (mm/s) 3. Nozzle temperature	1. Layer thickness decreases, the tensile strength of the material 2. Nozzle temperature increases, the tensile strength 3. Infill speed does not influence the tensile strength.
8.	Aditya Pulipaka, Ali Beheshti, Z. Shaghayegh Bag, Kunal Manoj Gide, [76]	PEEK (Poly Ether Ether Ketone)	FFF Process 1. Nozzle temp. 2. Platform temp. 3. Infill %, 4. layer height, 5. Print speed	1. Nozzle temperature and layer height have significant effects on surface roughness 2. UTS was significantly influence by platform temperature, layer thickness and nozzle temperature.

2.1. CONCULSION BASED ON THE LITERATURE REVIEW TABLE

This literature review table gives enormous information to how to use machine learning in the additive manufacturing. This material based literature review give also information about the material selection. Machine learning techniques have been employed in various aspects of FDM process optimization, aiming to enhance print quality, reduce defects, and optimize process parameters. It has been utilized to identify the optimal values for FDM process parameters such as nozzle temperature, print speed, layer height, and infill density. By analyzing large datasets of process parameter variations and corresponding print outcomes, machine learning models can determine the combinations that result in improved print quality, reduced defects, and reduced printing time. It have been developed to detect defects and assess the quality of FDM-printed parts.

2.2. RESEARCH GAPS

Based on the literature survey, it was discovered that the ensemble machine learning technique has not been used to predict the surface roughness in AM with advanced PLA+ material which has following benefits over standard PLA.

1. PLA+ has high strength, as compared to standard PLA polymers. Researchers have focused only on PLA, ABS, PEEK, and other polymer materials.

2. PLA+ has higher heat resistance as compared to standard PLA polymers.

3. Advanced polymers are used in the aerospace and automobile industries because of their high mechanical properties.

2.3. RESEARCH OBJECTIVES

This work has two distinct objectives. The first objective is to investigate the outcome of FDM process parameters on the surface roughness of PLA+ polymer. The second objective of this work is to predict the surface roughness of the samples by using machine learning.

Based on the literature gap, some important research objectives have been identified that

- To obtain better surface roughness by the FDM process in PLA+ polymer material.
- To study the appropriate material characterization of the manufactured polymer material, is it amorphous or crystalline.
- To develop better machine learning model to predict the surface roughness of the 3D-printed samples
- To analyze the behavior of surface roughness in nozzle temperature, printing speed, layer height, and infill density
- To study the micro hardness of the material in different parameters

CHAPTER 3.

RESEARCH METHODOLOGY

Research methodology is the step by step procedure of the working plan to understand the whole research objective by the flow charts see in figure 3.1.
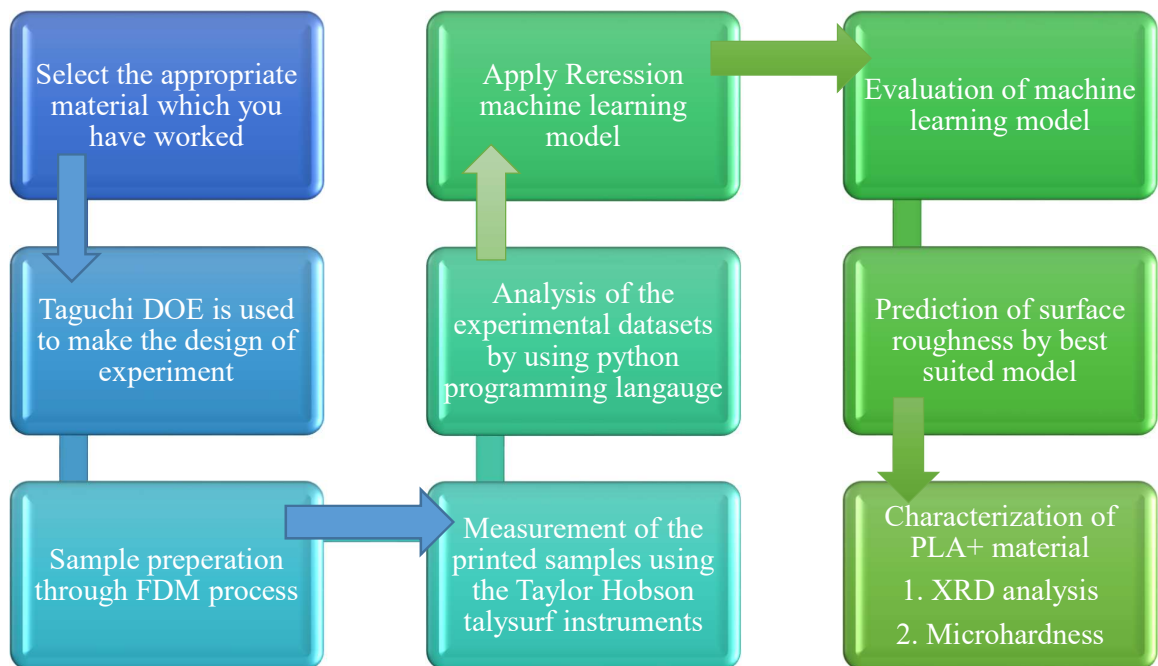
Figure 3.1: Research methodology flowcharts

3.1. MATERIAL

PLA and PLA+ are two types of 3D printing filaments that are widely used. PLA is a biodegradable and environmentally friendly material that is typically derived from corn starch or sugarcane. On the other hand, PLA+ is an advanced version of PLA that boasts enhanced physical properties like increased strength, durability, and heat resistance. Numakers Company procures the PLA+ material for all experimental work. PLA is crafted from natural and renewable resources such as sugarcane or cornstarch. To enhance its strength and durability, PLA+ is created by adding substances like carbon

fiber, metal particles, or other polymers see in figure 3.2. The result is a stronger and more durable material that can withstand higher stresses without breaking or cracking. Polylactic acid (PLA) is an environmentally friendly, thermoplastic aliphatic polyester that can be broken down by natural processes. It has the chemical formula $(C_3H_4O_2)n$ and is derived from renewable resources, specifically plant-based materials. On the other hand, reinforced polylactic acid (PLA+) is an enhanced and optimized thermoplastic filament material. It exhibits exceptional toughness, surpassing the strength of conventional PLA available in the market by a factor of ten.

PLA+ is particularly useful for printing objects that require more strength, durability, and resilience, and it retains its shape and physical properties even at temperatures up to 90 degrees Celsius. Its improved adhesion properties make it less prone to warping and ideal for printing large objects.
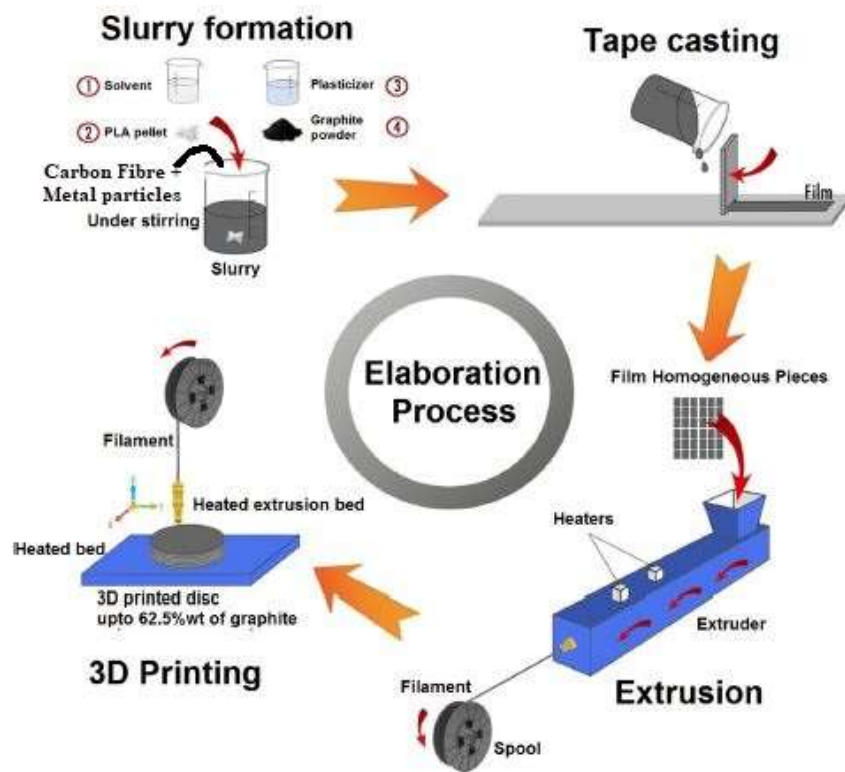
Figure 3.2: Geometry of material formation with 3d printing [77]

Additionally, PLA+ has best layer sticking and less shrinkage with less warpage than PLA, which change to a printed object that is closer to the same size and shape, with less warping or distortion during the 3D printing. Finally, PLA+ has a matte finish due to the natural additives in the material [78]–[81]. Both PLA and PLA+ are great options for 3D

printing. PLA is suitable for general-purpose printing, whereas PLA+ is more appropriate for printing objects that require greater strength, durability, and resistance to heat. PLA+ has enhanced properties compared to PLA as (shown in table 3.1), such as improved strength, durability, and heat resistance, making it the preferred material for printing high-performance objects. However, it is slightly more difficult to print with than PLA, and it is also more expensive due to the added additives.

Table 3.1: Comparison of mechanical property of PLA and PLA+ [82] - [83] **.**

Property	PLA	PLA+
Tensile strength	40 – 60 MPa	60 – 80 MPa
Elongation at Break	6 – 8%	4 -5 %
Young's Modulus	3 GPa	3.5 – 4 GPa
Density	1.24 – 1.27 g/cm^3	1.24 – 1.27 g/cm^3
Melting Point	160 – 180 ℃	190 – 220 ℃
Glass Transition Temperature	60 – 65 ℃	65 – 70 ℃
Heat Deflection temperature	50 – 60 ℃	80 – 100 ℃
Print Bed Temperature range	20 – 60 ℃	40 – 60 ℃
Print speed	50 -80 mm/s	40 – 60 mm/s
Layer Height	0.1 – 0.3 mm	0.1 – 0.4 mm
Shrinkage	Low	Very Low
Warping	Low	Very Low

PLA+ is a thermoplastic polymer that is commonly utilized in fused deposition modeling. It is an eco-friendly material that is fully biodegradable and produced from renewable resources obtained from corn starch fermentation. Additionally, it is cost-effective and offered in a range of colors. References [79]–[81] provides information on the properties of PLA. In FDM, the print quality can be impacted by several process parameters, including layer thickness, nozzle temperature, ,print speed, infill density, print orientation, shell thickness, and printing pattern. Only the parameters that directly affect surface roughness and mechanical properties are considered, which includes layer thickness, infill density, and nozzle temperature. These parameters, along with their corresponding levels for an FDM 3D printer with a 0.4 mm nozzle diameter, are chosen

using trial-and-error models. Table 3.2 presents the selected process parameters which i have worked in the whole prediction of surface.
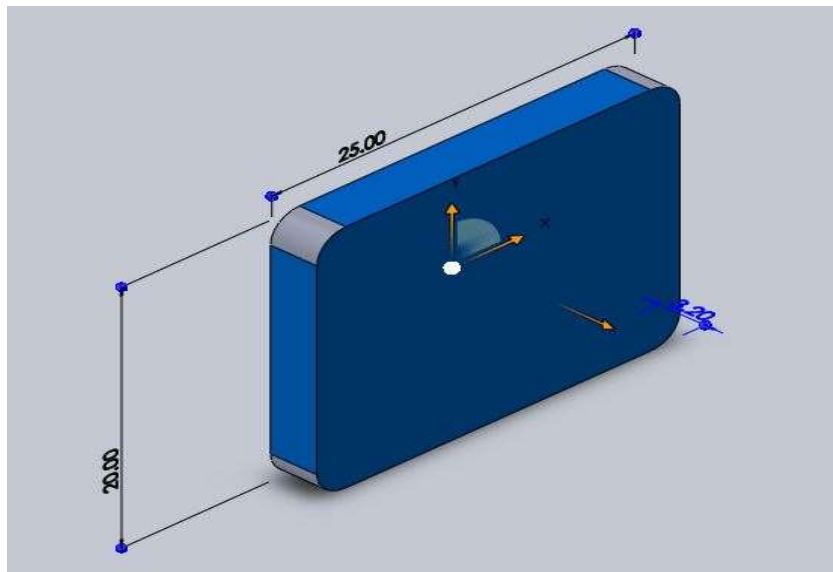
Figure 3.3: Schematic Diagram 3D sample parts with Geometry 25x20x3.2 mm³.

The experiment keeps all other parameters at a constant value while focusing on layer thickness, infill density, and nozzle temperature as the main process parameters. The printing speed, traveling speed, printing pattern, and shell thickness are also set to predetermined values. No supports are needed for printing the CAD models, so they are disabled. An orthogonal array (OA) is generated using MINITAB L25 software, which uses a 5-level Taguchi design with 5 factors. The L25 design is selected, resulting in a 5x5 array presented in Table 3.2. The specimens developed in a SolidWorks CAD model have dimensions of 25*20*3.2 mm³. See in figure 3.3.

3.2. TAGUCHI DESIGN OF EXPERIMENT

Genichi Taguchi developed the Taguchi method, which aims to reduce process variation through a robust design of experiment and produce very high-quality products at a low cost for manufacturers. The method involves using a taguchi orthogonal array to organize the parameters that affect the process and the dimensions at which they are varied.

The Taguchi method differs from the factorial design in that it only tests pairs of combinations, rather than all possible combinations. This approach is useful for identifying which factors have an impact on product quality while minimizing the amount

of experimentation required, thereby saving time and resources. The proposed experimental design by Taguchi is discussed in reference [84]. The Taguchi Orthogonal Array (OA) design is a fractional-factorial model that ensures all levels and factors are equally considered. This allows for independent evaluation of factors, despite the functionality of the design. The Taguchi orthogonal array design L25 chosen in [85].

Table 3.2: Control factors and different levels used for the Experiments

Parameters	L1	L2	L3	L4	L5
Printing Speed	50	60	70	80	90
Nozzle Temperature	200	207.5	215	222.5	230
Infill Density %	35	40	45	50	55
Layer Height	0.12	0.14	0.16	0.18	0.20

After applying the DOE these different levels and factors gives a table 3.3. The table is have 4 different parameters have printing speed, Infill density, and Nozzle temperature and layer height.

3.3. SAMPLE PREPERATION THROUGH FDM PROCESS

FDM is widely recognized as one of the most popular and extensively used additive AM techniques. It is a rapid prototyping (RP) technology that finds widespread industrial application due to its ability to construct complex functional parts efficiently. The FDM process involves the sequential deposition of thermoplastic filament, which is continuously supplied from a spool.

In FDM, the thermoplastic filament passes through a heating element within the liquefying head. Once a continuous supply of filament is available, it is heated until it reaches a semi-liquid phase. The liquefied thermoplastic material is then extruded through an extrusion nozzle onto the printing bed or platform. The filament is heated to its melting point and gradually deposited in layers to form the desired 3D model. This process is illustrated in Figure 3.4. The advantage of FDM lies in its ability to create intricate geometries with functional features, all while minimizing production time. The versatility and relative simplicity of the FDM technique contribute to its popularity across various industries. It allows for the fabrication of parts using a wide range of thermoplastic materials, making it suitable for diverse applications.

Table 3.3: Taguchi L25 orthogonal array

Exp No.	PS	NT	ID	LH
1	50	200	35	0.12
2	50	207.5	40	0.14
3	50	215	45	0.16
4	50	222.5	50	0.18
5	50	230	55	0.2
6	60	200	40	0.16
7	60	207.5	45	0.18
8	60	215	50	0.2
9	60	222.5	55	0.12
10	60	230	35	0.14
11	70	200	45	0.2
12	70	207.5	50	0.12
13	70	215	55	0.14
14	70	222.5	35	0.16
15	70	230	40	0.18
16	80	200	50	0.14
17	80	207.5	55	0.16
18	80	215	35	0.18
19	80	222.5	40	0.2
20	80	230	45	0.12
21	90	200	55	0.18
22	90	207.5	35	0.2
23	90	215	40	0.12
24	90	222.5	45	0.14
25	90	230	50	0.16
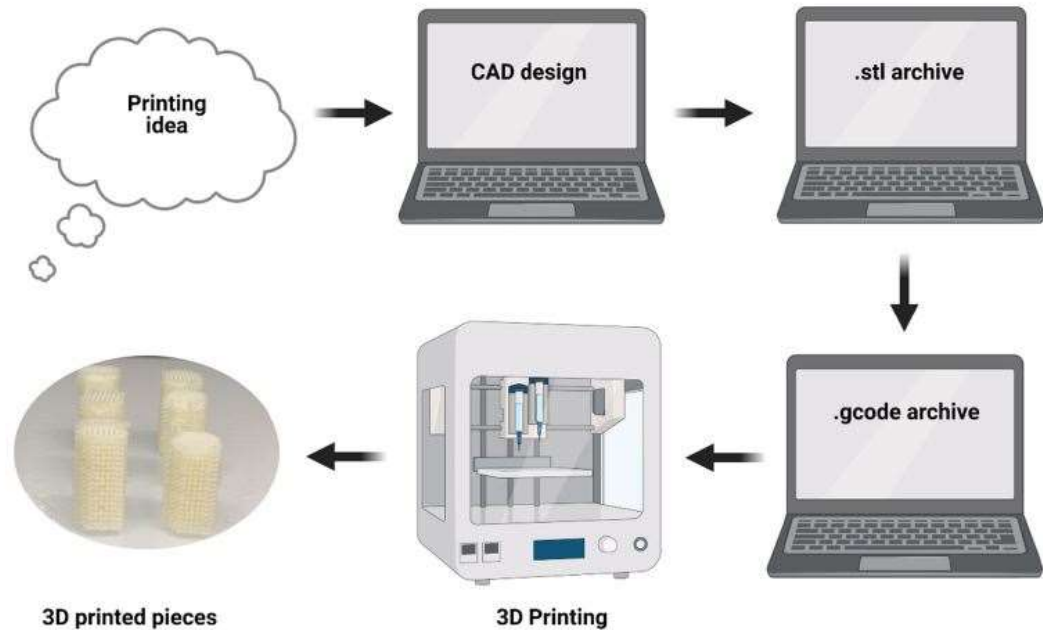
Figure 3.4: General summary of FDM [86]

The primary working principle of FDM is based on the behavior of semi-liquid thermoplastic filament materials when extruded from the printing nozzle. Instead of immediately solidifying upon extrusion, these semi-liquid thermoplastics fuse together to form a particular layer under construction. This fusion occurs before the material cures and solidifies into a stacked part composed of multiple layers, all at the ambient temperature surrounding the process.

FDM offers several benefits, including its simplicity, high-speed printing capability, and low cost. However, there are certain drawbacks associated with the technique. These include process parameter-dependent mechanical properties, resulting in anisotropic characteristics of the printed parts. The surface finishing of FDM parts tends to be poor, and the layer-wise appearance of the part is noticeable. Furthermore, FDM is limited to using thermoplastic polymers as printing materials due to the requirement of thermoplasticity for successful 3D printing. Achieving optimal part quality and mechanical properties in FDM requires the proper selection and optimization of process parameters. This is crucial for making FDM suitable for mass production and gaining acceptance in industries. The key steps involved in the FDM process include creating a CAD model, converting it into STL format, slicing the STL into thin layers, layer-by-layer construction of the part, and finally, cleaning and finishing.

For functional applications, important characteristics of FDM parts include dimensional accuracy, surface roughness, and strength. Manufacturing time is also a significant factor from an economic standpoint. However, achieving the desired characteristics in fabricated parts can be challenging without a thorough understanding of the impact of process variables. Therefore, optimizing process parameters becomes essential to achieve the desired quality characteristics in FDM-printed parts.

In the context of metal polymer composites, recent research focuses on analyzing various FDM process parameters such as layer thickness, percentage infill, bed temperature, and others. These parameters have a significant influence on the mechanical characteristics of FDM-printed metal polymer composites. In this chapter, the analysis of important printing factors impacting the mechanical characteristics of such composites is based on recent references. Specifically, the layer height, printing speed, nozzle temperature, and infill density are among the four FDM process parameters examined in relation to their effects on the surface roughness.

3.3.1. Layer height

In Fused Deposition Modeling (FDM), layer height refers to the thickness of each individual layer of material that is deposited during the 3D printing process. It is one of the key parameters that can be adjusted when setting up a print job. When using an FDM 3D printer, the printing nozzle moves along the X and Y axes, while the build platform moves down incrementally in the Z direction after each layer is deposited. The layer height determines the vertical distance between each layer. Choosing the appropriate layer height is important as it can affect the overall print quality and printing time.

Nozzle Diameter: The layer height should be chosen in relation to the diameter of the printer's nozzle. As a general guideline, it is recommended to use a layer height that is equal to or slightly smaller than the nozzle diameter. For example, if you have a 0.4 mm nozzle, a layer height of 0.2-0.3 mm would be suitable. Thinner layer height adds to increased tensile strength owing to stronger adhesion between layers, according to the testing results.

3.3.2. Printing speed

Printing speed in FDM refers to the rate at which the 3D printer extrudes and deposits material to create the desired object. It is typically measured in millimeters per second

(mm/s) or millimeters per minute (mm/min). The printing speed affects the time it takes to complete a print job and can also impact the quality of the final object

Print Quality vs. Speed: Increasing the printing speed can reduce the overall print time but may lead to compromises in print quality. High-speed printing can result in less precise details, increased vibrations, and potential issues like layer shifting or poor adhesion. It's crucial to find the right balance between speed and quality based on your specific requirements.

3.3.3. Nozzle temperature

In Fused Deposition Modeling (FDM), nozzle temperature refers to the temperature of the printing nozzle or extruder. It is a critical parameter in 3D printing as it directly affects the melting and flow characteristics of the filament material. The filament, typically made of thermoplastic material, is fed into the printer's extruder. The extruder contains a heating element that melts the filament, and the molten material is then deposited layer by layer to create the object. The nozzle temperature determines how hot the extruder needs to be to achieve proper melting and flow of the filament. Nozzle temperature can influence various aspects of the printed object, including layer adhesion, strength, and surface finish. Some materials require higher temperatures for proper bonding between layers, while others may have lower temperature requirements. Experimentation and adjusting the temperature within the recommended range can help optimize print quality.

3.3.4. Infill Density

Infill density, in the context of Fused Deposition Modeling (FDM) or 3D printing, refers to the amount of internal structure or material inside a printed object. It represents the density of the pattern or structure that is printed within the solid exterior shell of the object. When printing a 3D model, the software used to slice the model into printable layers allows for adjusting the infill density. The infill is typically represented as a pattern of lines, grids, or other geometric shapes that are printed within the walls of the object. Infill density affects the strength and durability of the printed object. Higher infill densities result in a more solid internal structure, increasing the strength of the object. However, higher infill densities also consume more material and can increase print time. Supports and Stability: Infill density plays a role in providing support and stability to the object. Higher infill densities can provide better support for overhanging or complex

geometries and reduce the likelihood of sagging or deformations during printing. It can also improve the overall stability and structural integrity of the object.

A total of 25 samples were printed according to the Taguchi L25 orthogonal array, as illustrated in Figure 3.6. These samples were printed using an Ender 3 3D printer, which is identify in Figure 3.5. The specifications of this 3D printer are provided in Table 3.4. To test the surface roughness of the PLA+ material printed part, the Taylor Hobson surface roughness tester equipment was used. The components that were fabricated underwent testing using the Taylor Hobson machine shown in Figure 3.7, which has a range of approximately 0.05 to 12.25 um and is used in battery connectivity operations. Before testing the fabricated parts, it was necessary to check whether the diamond tip connected to the stylus was straight or not. Additionally, the surface roughness of the given sample base plate, which measured 6 um, was examined. Surface roughness was tested in three different positions of the sample parts, and the average of all three positions was taken to determine the final surface roughness (Avg), as shown in Table 3.5.

Table 3.4: Specification of Ender-3 3D printer.

S.No.	Parameter	Type/Size
1	Bed size	235 * 235
2	Bed type	Heated
3	Max travel	X= 235, Y = 235. Z = 250
4	Nozzle size	0.4 mm
5	File supported	G code
6	Material Supported	PLA, PLA+, ABS
7	Display size	2.5 Inch
8	Max speed	120 mm/s
9	Power supply	220 – volt AC, 240Watt
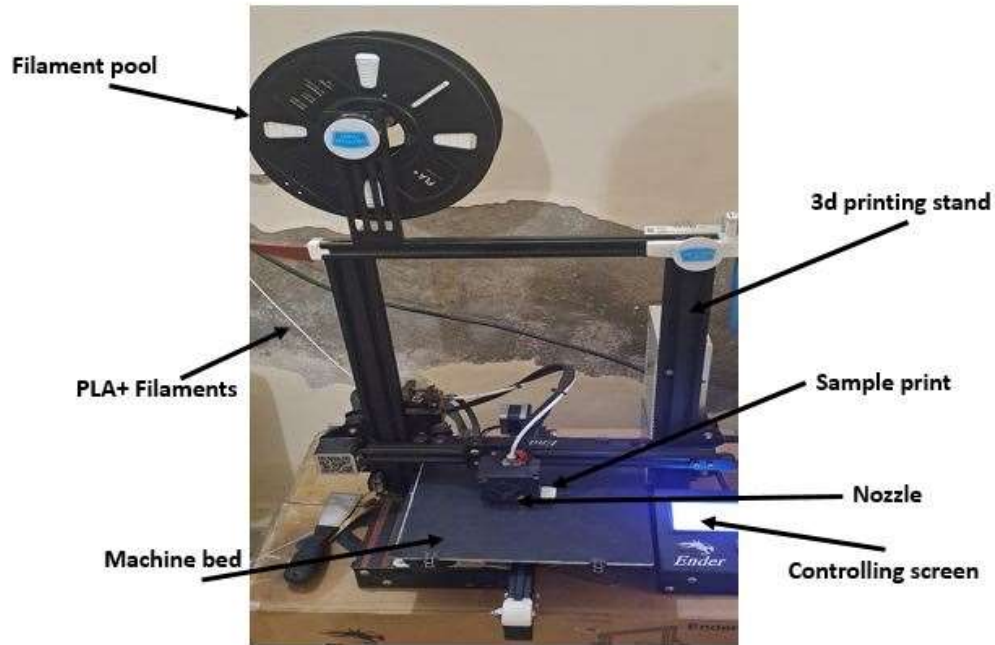
Figure 3.5: Ender-3 3D printer machine

Figure 3.6: 3d Printed sample parts

3.4. SURFACE ROUGHNESS MEASUREMENT BY TAYLOR HOBSON

Taylor Hobson is a well-known manufacturer of precision metrology instruments, including surface roughness measurement devices. Modeling (FDM) samples, I can provide you with a general overview of how surface roughness data is typically generated using such instruments. The resulting surface of an FDM sample can exhibit varying levels of roughness due to factors such as layering, material properties, and process parameters. To quantify and characterize the surface roughness of an FDM sample, a

Taylor Hobson surface roughness measurement instrument can be used. The TalySurf instrument has a resolution or least count of 0.1 nanometers (nm). This means that it can detect and display changes in surface roughness down to the nearest 0.1 nm increment. The resolution represents the smallest measurable unit of roughness that the instrument can reliably detect and quantify. These instruments typically employ a stylus-based measurement technique known as profilometry. Here are the general steps involved in generating surface roughness data using a Taylor Hobson instrument:

3.4.1. Preparation

The FDM sample is cleaned to remove any debris or contaminants that may affect the measurement. It is essential to ensure that the sample is stable and securely mounted to prevent any movement during measurement.

3.4.2. Calibration

The instrument needs to be calibrated before taking measurements. Calibration involves adjusting the instrument's settings, such as stylus force, scan length, and stylus radius, to ensure accurate and reliable measurements.

3.4.3. Measurement setup

The instrument is configured with appropriate measurement parameters based on the characteristics of the sample and the desired analysis. Parameters such as cutoff length, sampling length, and evaluation length are set to define the measurement area and determine the level of detail captured.

3.4.4. Measurement process

The instrument's stylus is brought into contact with the surface of the FDM sample. The stylus then traces across the sample surface, following a predetermined path or scanning pattern. As it moves, the stylus measures the vertical displacement of the surface, recording data points at regular intervals.

3.4.5. Data acquisition

The instrument captures the data points recorded by the stylus, which correspond to the height variations of the surface. The collected data is typically stored in a profile file or transferred to a computer for further analysis.

Data analysis: The surface roughness data is analyzed to extract various parameters that quantify the surface texture. The surface roughness data, along with the calculated parameters, can be presented in a graphical format or as a numerical report. The data can be used to evaluate the quality of the FDM sample, compare different samples or processes, or ensure compliance with specific surface roughness requirements.

Table 3.5: Surface roughness result by Taylor Hobson

| Exp No.	PS	NT	ID	LH	SR (Ra1)	SR (Ra2)	SR (Ra2)	SR Average
1	50	200	35	0.12	4.24	4.3	4.08	4.20
2	50	207.5	40	0.14	5.72	5.86	5.25	5.61
3	50	215	45	0.16	6.50	6.31	6.21	6.34
4	50	222.5	50	0.18	7.21	7.88	7.46	7.51
5	50	230	55	0.2	9.54	9.36	8.94	9.28
6	60	200	40	0.16	6.44	7.1	6.32	6.62
7	60	207.5	45	0.18	7.31	7.84	8.44	7.86
8	60	215	50	0.2	8.41	8.19	8.75	8.45
9	60	222.5	55	0.12	4.12	4.365	4.62	4.4
10	60	230	35	0.14	5.84	5.7	5.81	5.78
11	70	200	45	0.2	8.89	9.12	9.4	9.13
12	70	207.5	50	0.12	4.14	4.68	4.84	4.55
13	70	215	55	0.14	5.94	5.34	6.24	5.84
14	70	222.5	35	0.16	6.34	6.84	6.94	6.70
15	70	230	40	0.18	8.154	8.54	8.21	8.30
16	80	200	50	0.14	6.25	6.32	6.05	6.20
17	80	207.5	55	0.16	7.45	7.64	6.84	7.31
18	80	215	35	0.18	8.54	8.89	8.24	8.55
19	80	222.5	40	0.2	7.55	7.3	7.95	7.6
20	80	230	45	0.12	5.15	5.89	5.25	5.43
21	90	200	55	0.18	9.32	9.75	8.95	9.34
22	90	207.5	35	0.2	10.25	9.98	9.84	10.02
23	90	215	40	0.12	7.1	6.84	6.35	6.76
24	90	222.5	45	0.14	6.65	6.9	6.25	6.6
25	90	230	50	0.16	8.21	8.75	8.1	8.35
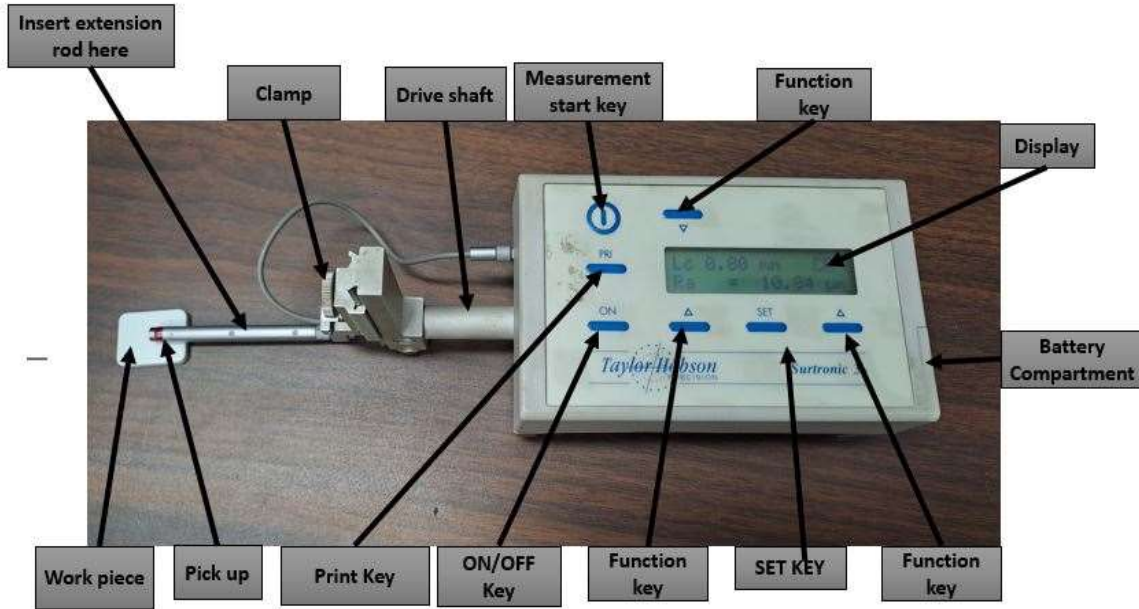
Figure 3.7: Taylor Hobson surface roughness tester with printed sample parts

Surface roughness is measured by three points in the samples and after that taken the average of all the three surface roughness of the 3d printed samples parts which is shown in the table no. 3.5.

3.5. DATA PREPROCESSING

Preprocessing data in machine learning refers to the steps and techniques applied to the raw data before it is used to train a machine learning model. The purpose of data preprocessing is to transform and prepare the data in a format that is suitable for the machine learning algorithms, improving the accuracy and efficiency of the model. The implementation of various machine learning (ML) approaches typically follows a standard workflow, as depicted in Figure 3.8, comprising five steps to model a problem effectively.

Step 1: Data Collection involves gathering a dataset consisting of samples. Each sample includes input variables that describe the problem being modeled, and in the case of supervised learning algorithms, corresponding numeric output target values for regression models. This step is crucial for providing the necessary data to train and evaluate ML models.

Step 2: Data Pre-processing focuses on preparing the dataset for ML algorithms. It involves tasks such as data cleansing and formatting. Data cleansing involves removing or repairing incorrect or missing data, reducing noise, and applying data augmentation techniques to create a more balanced dataset, especially for classification tasks. Feature selection, transformation, and extraction/engineering are applied to enhance the dataset. Unnecessary features may be removed, remaining features can be transformed through normalization or scaling, and new features can be extracted from the input data.

Step 3: Model Training focuses on selecting suitable parameters for the learning algorithm and executing the training process. The algorithm analyzes the training data to discover patterns that map input features to the corresponding output target. Feature selection involves selecting a subset of relevant features from the dataset. This helps reduce the dimensionality of the data, removing irrelevant or redundant features, and improving the model's efficiency and interpretability. The output of this step is an ML model that captures the learned patterns and can generate accurate predictions when presented with new input samples. The dataset is typically split into training and testing sets. The training set is used to train the machine learning model, while the testing set is used to evaluate its performance. This helps assess the model's generalization ability and prevent overfitting.

Step 4: Model Performance Evaluation involves assessing the generated model's performance. It is done by measuring its responses to the testing dataset using performance metrics specific to the problem at hand. This step helps determine the model's effectiveness and provides insights into its strengths and weaknesses.

The specimens were manufactured with FDM 3D printing and tested for surface roughness on a Taylor Hobson surface roughness tester. Different machine learning is used to predict the surface roughness of the 3D printed parts, which show different results in the training and testing datasets.
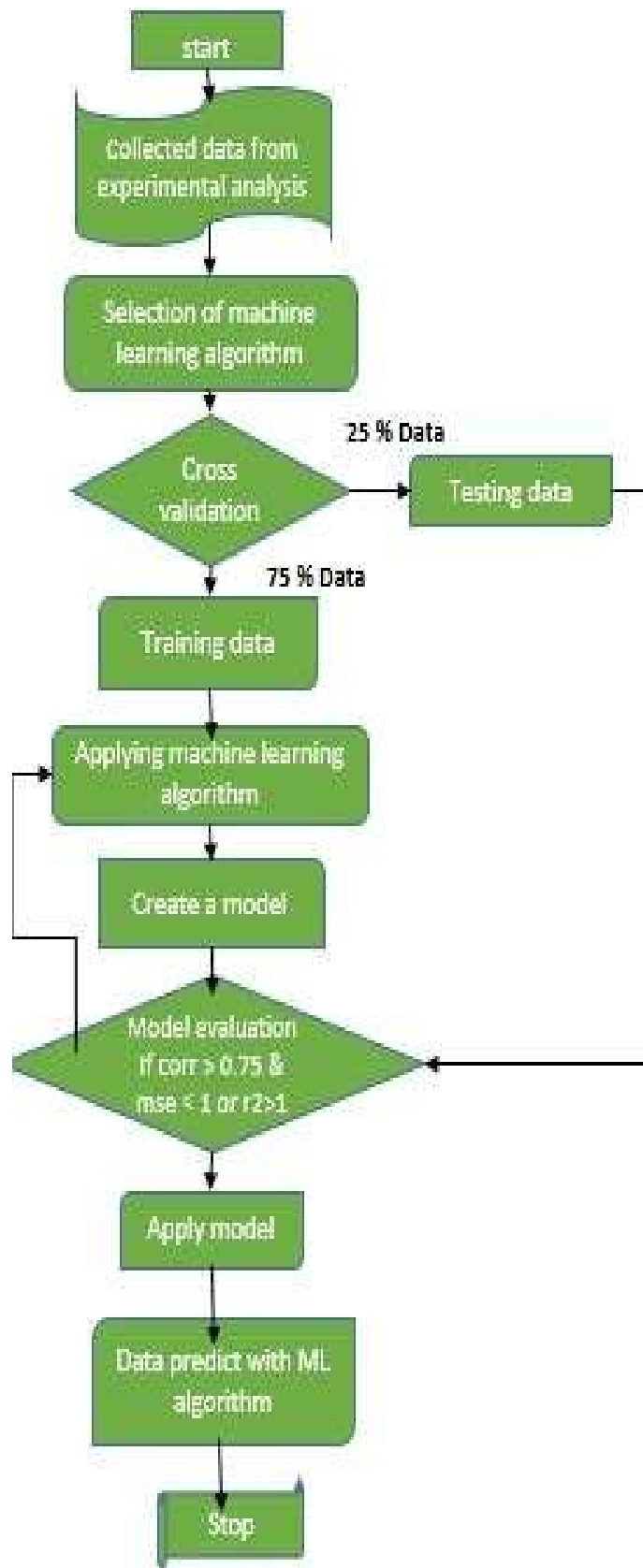
Figure 3.8: Working procedure of different ML created by flow chart

3.6. MACHINE LEARNING ALGORITHM (REGRESSON ANALYSIS)

Regression analysis is a set of statistical techniques used to determine the relationship between a response variable and one or more predictor variables

3.6.1. Linear Regression

The most commonly used type of regression analysis is linear regression. It involves selecting a line, or new complex linear combination, that best fits the experimental data based on a set of mathematical formula (illustrate in figure 3.9). Linear regression is the oldest and most widely used category of regression analysis [87]. In a linear regression model, there is a specific form that must be followed. The model is linear when it holds a constant and a parameter multiplied by each independent variable, which are used to predict the dependent variable. The equation for linear regression is shown below:

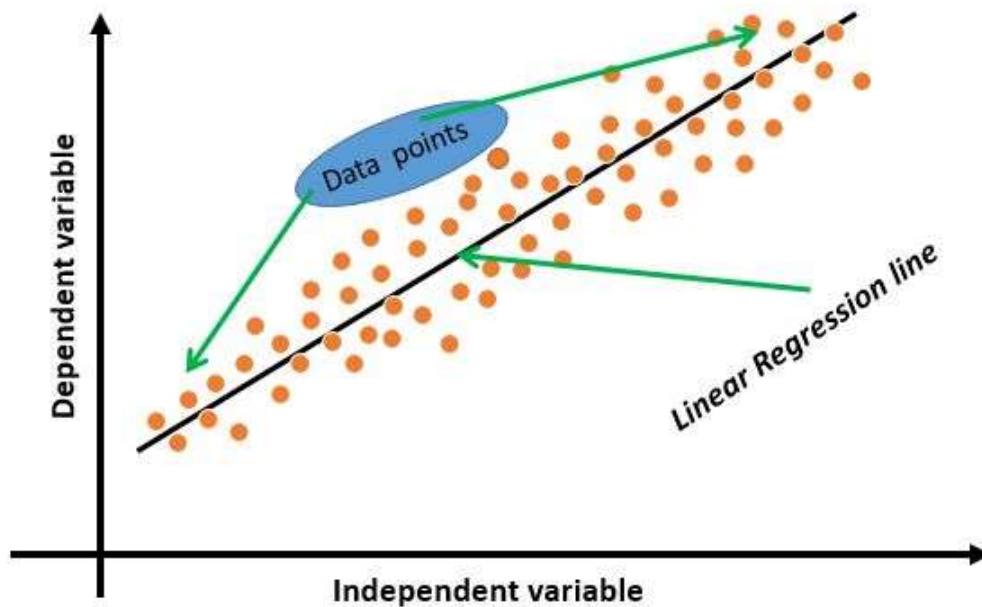**Figure 3.9: Schematic diagram of linear regression** [88]

$$y = a_0 + a_1x_1 + a_2x_2 \ldots + a_mx_m\epsilon \hspace{4cm} \text{Eq2}$$

Here, y is the dependent variable, x1...xm are the independent variables, a0 is the intercept of the line, and a1...am are the regression coefficients. The value of ϵ represents the random error. The training datasets for the linear regression model representation

include values for both the x and y variables. All the linear regression code is done in jupyter notebook and code snippet is shown in appendix I.

3.6.2. Support Vector Regressor (SVR)

Support Vector Machines (SVM) is a machine learning technique rooted in statistical learning theory and the principle of structural risk minimization. To classifying patterns and performing non-linear regression. SVR is the application of SVM to non-linear regression problems. Its main idea is to use a kernel function to map non-linear data points to a good-dimensional space and fit them to a hyperplane [28], [89]. By minimizing the error distance between data points and a hyperplane, Support Vector Machines (SVM) facilitate the description and prediction of non-linear relationships. (see in figure 3.10)
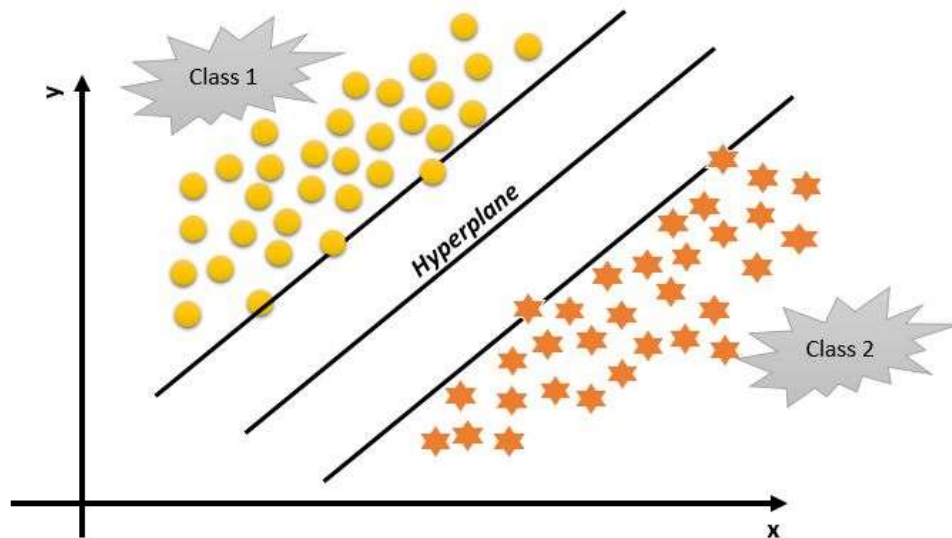
Figure 3.10: Schematic diagram of svm [90]

The algorithm achieves this by utilizing a kernel function that allows for the transformation of the original feature space into a higher-dimensional space. In this higher-dimensional space, the data points can be separated by a hyperplane, even if the original feature space is not linearly separable. [5]. All the support vector regression code is done in jupyter notebook and code snippet is shown in appendix II.

3.6.3. Random Forest Repressor

Random Forest (RF) is an ensemble learning algorithm introduced by Breiman in 2001, which has gained popularity in machine learning. This technique constructs a forest of decision trees by utilizing bootstrap sampling. Each decision tree in the ensemble is independent and contributes to the final prediction (refer in figure 3.11). Despite its simplicity, Random Forest has been widely acknowledged for its excellent performance across various types of tasks. Random Forest is particularly effective in regression tasks. To build a regression tree, two crucial criteria are employed: a splitting criterion, which determines how the tree branches based on input features, and a stopping criterion, which defines when the tree growth should stop.
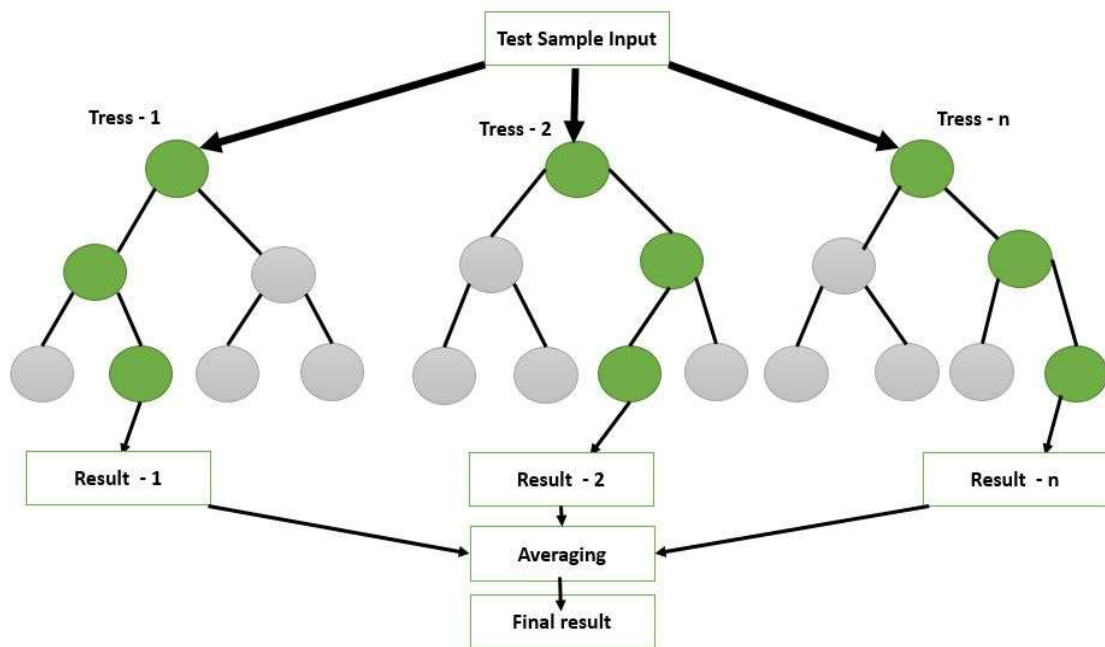
Figure 3.11: Schematic illustration of random forest regressor [91]

The Random Forest algorithm leverages the concept of combining multiple decision trees to improve prediction accuracy and robustness. Each decision tree in the ensemble is trained on a different subset of the data, obtained through bootstrap sampling. This randomness in data sampling, combined with the independence of the trees, helps to reduce overfitting and improve the overall generalization performance of the model. The implementation of Random Forest can be done using various programming environments, such as Jupyter Notebook, where the code can be written and executed. (see in appendix III.)

3.6.4. Gradient Boosting Regression tree

Gradient Boosting regression (GBR) is a ML algorithm that joins multiple decision trees to create a stronger model. The decision trees are the core models of the algorithm, and GBR uses a statistical technique called boosting to improve the performance of the decision tree models. The boosting approach involves incrementally building new decision trees by reducing the current residuals (refer in figure 3.12). In the original Boosting algorithm, each sample is assigned equal weight at the beginning of the algorithm, and all the base learners are equally important [92].

The Gradient Boosting regression (GBR) algorithm is an ensemble boosting method that uses decision trees as core models. Its goal is to joins a set of models to build a single strong machine model. In GBR, the technique of boosting incrementally constructs new decision trees by reducing the current residuals.
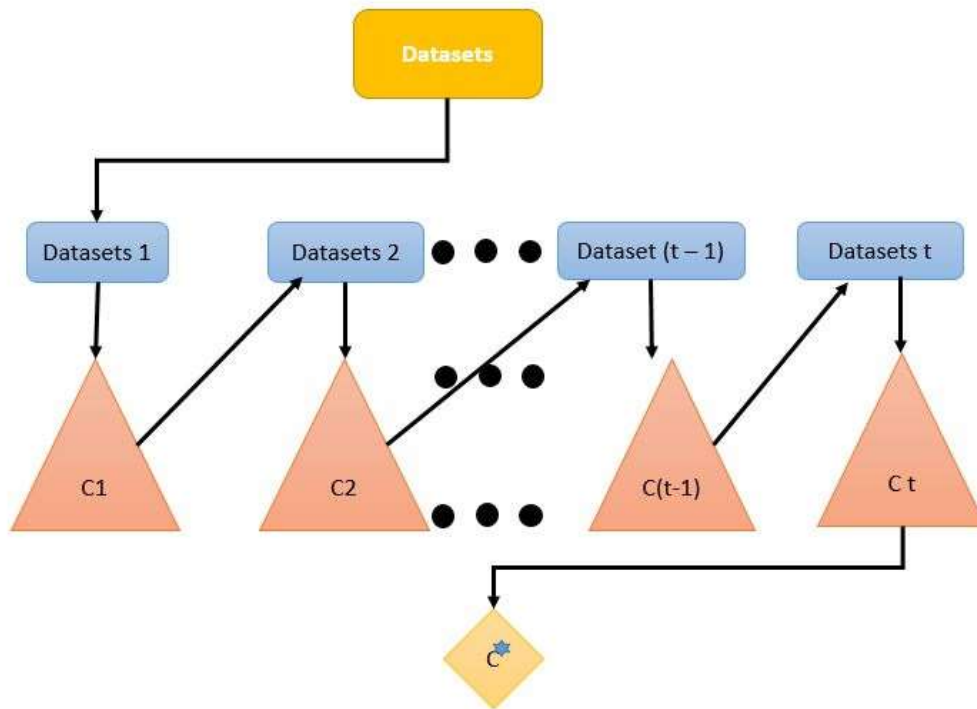

Figure 3.12: Schematic diagram on boosting technique [93]

Unlike the original Boosting algorithm, in GBRT, incorrectly predicted samples are given a higher weight in the next step, while correctly predicted samples are given a lower weight [94]. All the Gradient boosting regression code is done in jupyter notebook and code snippet is shown in appendix IV.

3.7. EVALUATION OF MACHINE MODEL

Evaluating a regression machine learning model involves assessing how well the model performs in predicting continuous numeric values. There are several commonly used evaluation metrics to measure the act of regression models. Here are some key metrics:

3.7.1. Mean Squared Error (MSE)

The average of the squared variations between the predicted and actual values is computed by MSE. Lower values reflect greater performance because it calculates the average squared difference between the expected and true values. However, MSE is sensitive to outliers.

$$MSE = \frac{1}{n}\sum_{i=1}^{n}(Y_i - Y^{\wedge}_i)^2 \qquad\qquad \text{Eq. 3}$$

MSE =mean squared error, n = number of data points, Y_i = observed values, $Y^{\wedge}_i$= pred value

3.7.2. Root Mean Squared Error (RMSE)

RMSE is the square root of the MSE. It gives an accountable metric in the same size as the target variable, making it easier to understand the magnitude of the errors [95].

$$RSME = \sqrt{\frac{\sum_{i=1}^{N}||y(i)-y^{\wedge}(i)||^2}{N}} \qquad\qquad \text{Eq. 4}$$

Where N = number of data points, y(i) = Ith measurement and $y^{\wedge}(i)$ = corresponding prediction

3.7.3. Mean Absolute Error (MAE)

The Mean Absolute Error (MAE) is a metric used to evaluate the performance of a prediction model. It calculates the average absolute difference between the predicted values and the actual values. Unlike other metrics, such as Mean Squared Error (MSE), MAE focuses on the magnitude of errors rather than their squared values [95].

$$MAE = \frac{\sum_{i=1}^{n}|y_i-x_i|}{n} \qquad\qquad \text{Eq. 5}$$

MAE = mean absolute error,

y_i = prediction,

x_i = true value

n = total number of data points

3.7.4. R-squared (R²) or Coefficient of Determination

R-squared measures the proportion of the variance in the target variable that is forecasted from the independent variables used in the model. It ranges from 0 to 1, where 1 indicates that the model explains all the variability in the target variable. However, R-squared can be biased when adding more independent variables to the model [96].

$$R^2 = 1 - \frac{SSR}{SST} = 1 - \frac{\Sigma(\widehat{y_i} - \bar{y})^2}{\Sigma(y_i - \bar{y})^2}$$

Eq. 6

SSR = sum squared error, SST = total sum of squares,

When evaluating a regression model, it's important to take the specific characteristics of the experimental problem, the distribution of the data, and the aim of the analysis. It's also useful to compare the model's performance with baseline models or other algorithms to determine its effectiveness in making accurate predictions. After the evaluation of the machine model a user interface (see in appindex V) is created by the tinkter library which predict the surface roughness by inputting the variable parameters.

3.8. CHARACTERIZATION OF PLA+ MATERIAL

3.8.1. X-ray Diffraction

X-ray diffraction (XRD) is a technique used to analyse the crystal structure and molecular arrangement in a material. When analyzing the XRD pattern of a PLA+ polymer, several factors can influence the results, including the specific composition of the polymer, processing conditions, and any additives used. XRD results typically show characteristic diffraction peaks that correspond to the arrangement of polymer chains or crystalline regions within the material. To obtain the XRD result of a specific PLA+ polymer, you would need to conduct the experiment by preparing a sample of the polymer which is shown in the figure 3.13, subjecting it to X-ray diffraction analysis, and interpreting the resulting diffraction pattern
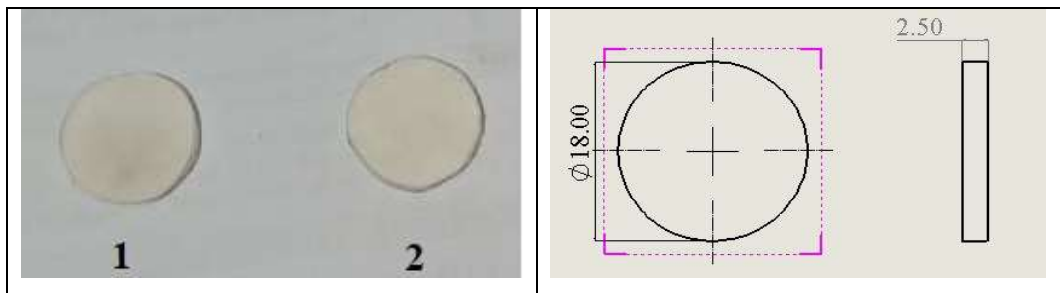

Figure 3.13: Schematic diagram of XRD samples in 18 mm diameter and 2.5 mm thickness

The samples used in this study were 3D printed using identical parameters, with a nozzle temperature of 220°C and a build platform temperature of 60°C. The printing process involved a 55% infill, where the interior of the printed object was filled with material, and a cubic fill pattern was used for each layer, aligning parallel to the axis of the object. To analyze the crystal structure of the printed samples, single crystal X-ray diffraction data was collected using a Bruker advanced D8 X-ray diffraction machine. The machine, depicted in (Figure 3.14) was operated at room temperature, scanning over a 2θ range from 2 to 70 with a step size of 0.05. The X-ray source employed in the machine was a graphite-monochromatic with a wavelength of λ=1.5406. To process the collected data, well-established computational procedures were utilized for data reduction. This involved performing corrections for Lorentz and polarization effects, followed by an empirical absorption correction based on a technique known as "multi-scan". These procedures helped obtain the structural factors necessary for further analysis and interpretation of the crystal structure of the printed samples.

Figure 3.14: Bruker advanced D8 XRD testing machine

3.8.2. Microhardness of PLA+ polymer material

Microhardness of PLA+ material involves evaluating the hardness characteristics of a specific type of PLA (Polylactic Acid) material that has been modified or enhanced with additives to improve its mechanical properties. Microhardness refers to the ability of a material to resist indentation or penetration by an indenter under a specific load. To Set the test parameters, including the test load and dwell time, based on the characteristics of the PLA+ material and the desired level of precision. Capture images or record the dimensions of the indents produced on the PLA+ material surface and measure the indentation. Calculate the microhardness values using the measured indentation dimensions and the test parameters. Microhardness is typically expressed in units of HV (Vickers hardness) or kg/mm². If conducting a comparative study or evaluating multiple samples, perform statistical analysis on the obtained microhardness data.

The microhardness test is usually used to illustrate the hardness of different polymer materials at small applied loads like 0.5 kgf (4.903N) with static indentations. In this investigation, the microhardness was measured at 0.5 kgf (4.903325 N) with a dwell time of 10 s. The indenter type is the Vickers diamond pyramid, model Struers Duramin – 40M (Delhi technological university). The Vickers hardness number (HV), is calculated according to the equation which is shown below [97]:

$$HV = 1.8544 \; \frac{p}{d^2}$$
Eq. 7

Where P = Applied load in kgf, d = an arithmetic mean of diagonals in mm and HV is the Vickers hardness number.

CHAPTER 4

RESULTS AND DISCUSSION

4.1. INTRODUCTION

The generated machine learning model considers a total of four input parameters, with surface roughness measurement serving as the output. The input data or features consist of the following printing parameters: printing speed, Infill Pattern (IP), nozzle temperature, and Layer Thickness (LT), with a raster angle of 0 degrees. These parameters were obtained through the experimental procedure outlined in the experimental work, which was then used to calculate the surface roughness output of the 3D printed sample parts. Figure 4.1, 4.2, 4.3 and 4.4 displays the correlation between the input and output variables of the experimental datasets, while Figure 4.5 shows the Heatmap correlation which is created using Python programming. After making the best fitted model also calculated the characterization of the PLA+ polymer material which check this polymer is amorphous or crystalline

4.2. EFFECT OF PRINTING PARAMETERS IN SURFACE ROUGHNESS

Layer height. Printing speed, nozzle temperature and Infill density all the four parameters shown different impact on the surface roughness which is shown in the figure 4.1, 4.2, 4.3 and 4.4. All the variation of the process parameters with surface roughness are shown in the figure. The layer height determines the thickness of each printed layer. A smaller layer height generally results in finer surface details and smoother surfaces. However, using a smaller layer height can increase print time and may require a higher level of printer precision and larger layer height shows large surface roughness. The extrusion temperature of the filament affects its flow and bonding characteristics. The temperature should be set within the recommended range for the filament material being used. Incorrect temperature settings can lead to under or over-extrusion, which can impact surface quality. The speed at which the printer moves during the printing process can impact surface roughness. Higher printing speeds may lead to rougher surfaces due to less time for the material to cool and solidify. Slower printing speeds generally result in smoother surfaces but can increase overall print time.
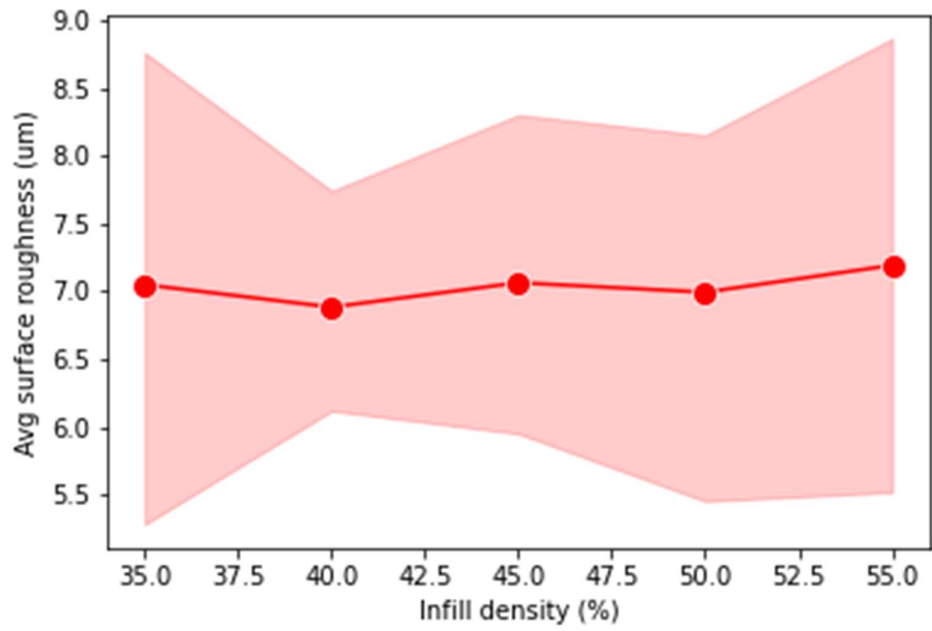
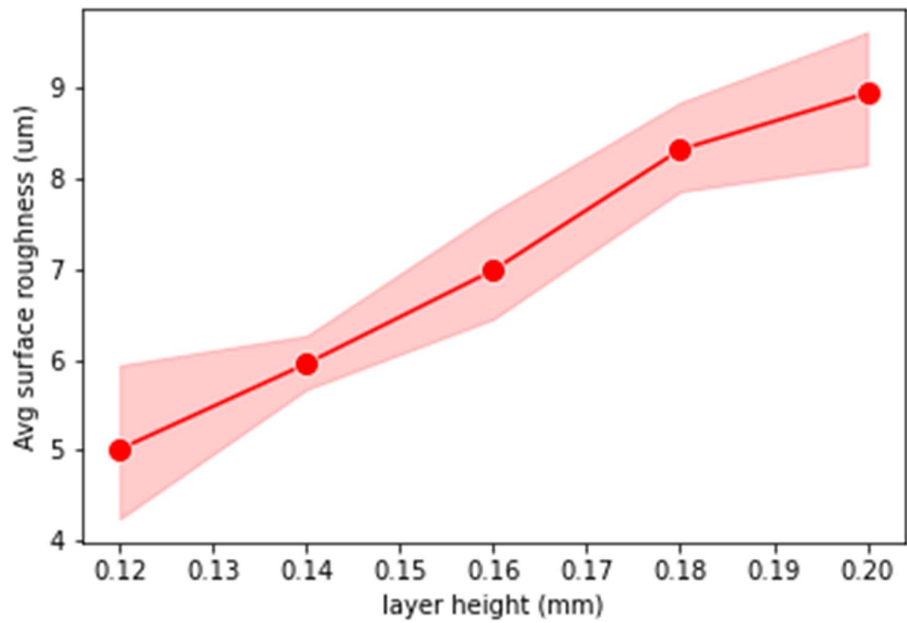**Figure 4.1: Variation of Surface roughness vs infill density**

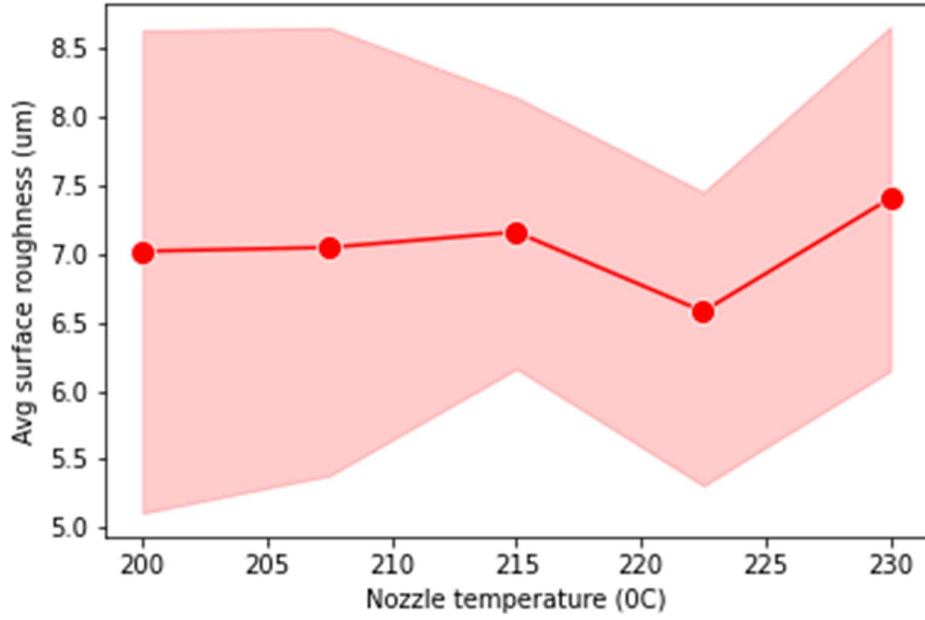**Figure 4.2: Variation of Surface roughness vs layer height**

Figure 4.3: Variation of Surface roughness vs Nozzle temperature
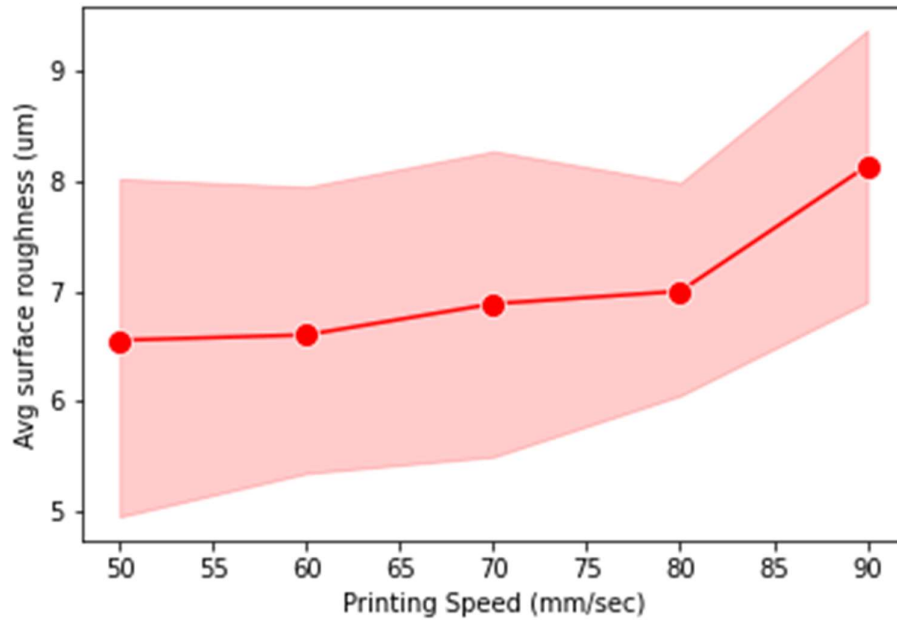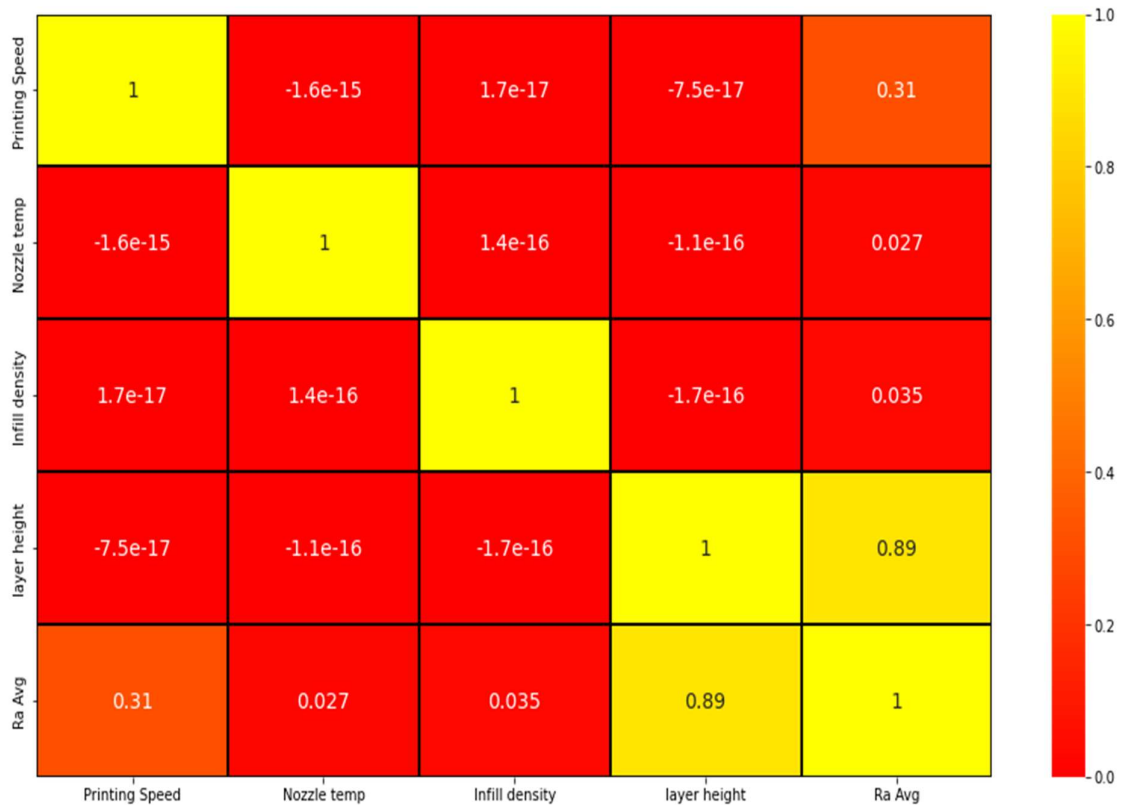

Figure 4.4: Variation of Surface roughness vs printing speed

Figure 4.5: Heatmap of correlation with surface roughness with other parameters

This heatmap gives the percentage of correlation of input features to the output features (Surface Roughness). This heatmap gives the correlation in percentage which is given below

1. Printing speed is 31% corr. With Ra
2. Nozzle temperature is 2.7% corr. with Ra
3. Infill density is 3.5% corr. with Ra
4. Layer height is 89% corr. With Ra

The correlation analysis reveals that layer height has a very strong correlation with surface roughness, at approximately 89%. Conversely, infill density and nozzle temperature have the least correlation with surface roughness. Infill density primarily affects tensile strength rather than surface roughness, as it fills the inside of the material in 3D printed parts. Nozzle temperature also has minimal correlation, as the melting temperature of the PLA+ polymer used in the experiment is around 200-230 degrees Celsius, as indicated on the filament coils purchased from the Numkers company. Given

these findings, we eliminated the two least correlated parameters, nozzle temperature and infill density, and focused on the highly correlated layer height parameter. The dataset was then split into training and testing sets, with 75% allocated for training and 25% for testing. The machine learning model was applied to the datasets.

4.3. ANALYSIS OF MACHINE LEARNING IN THE EXPERIMENTAL DATASETS

All the machine learning used one by one and check which one is best fitted results in my experimental datasets. And the result is shown in the table 4.1. Evaluation of machine learning also checked to identify which one's better machine model

Table 4.1: Training and testing result in different Ml algorithm

Machine Learning algorithm	Training score (%)	Testing score
Linear regression	85.0	84.29
Support vector machine	3.08	-3.099
Random forest repressor	94.45	95.45
Gradient Boosting regression	98.871	36.67

Random forest regression shows a better-fitted algorithm on training and testing datasets, which is shown in the above table 4.1 in all over the machine learning and also checking the evaluation of all 4 algorithms. To determine whether a machine learning regression model is good or not, you can use various evaluation metrics, such as MSE: which measures the average squared difference between the predicted and actual values. A lower value of MSE indicates a better model. R-squared (R2) score: It represents the proportion of variance in the target variable that is explained by the independent variables. A higher value of R2 indicates a better model. RMSE: It is the square root of MSE and represents the average distance between the predicted and actual values. A lower value of RMSE indicates a better model.

Random forest regressor is minimum mse 0.1255 and maximum r2_Score with 0.9685 as compared to the linear regression and the other two algorithms give more error as compared to the random forest, the overall best algorithm is random forest regressor because it has better training accuracy, testing accuracy, less mean squared error and also great r2_score of all the ML algorithm. After applying the best ML model make a user interface to predict the surface roughness by using the saved model.

All the actual and predicted data are shown by the graph in Figure 4.6 in different machine learning algorithms. This graph shows a graphical representation of all detailed understanding of the actual and predicted data.
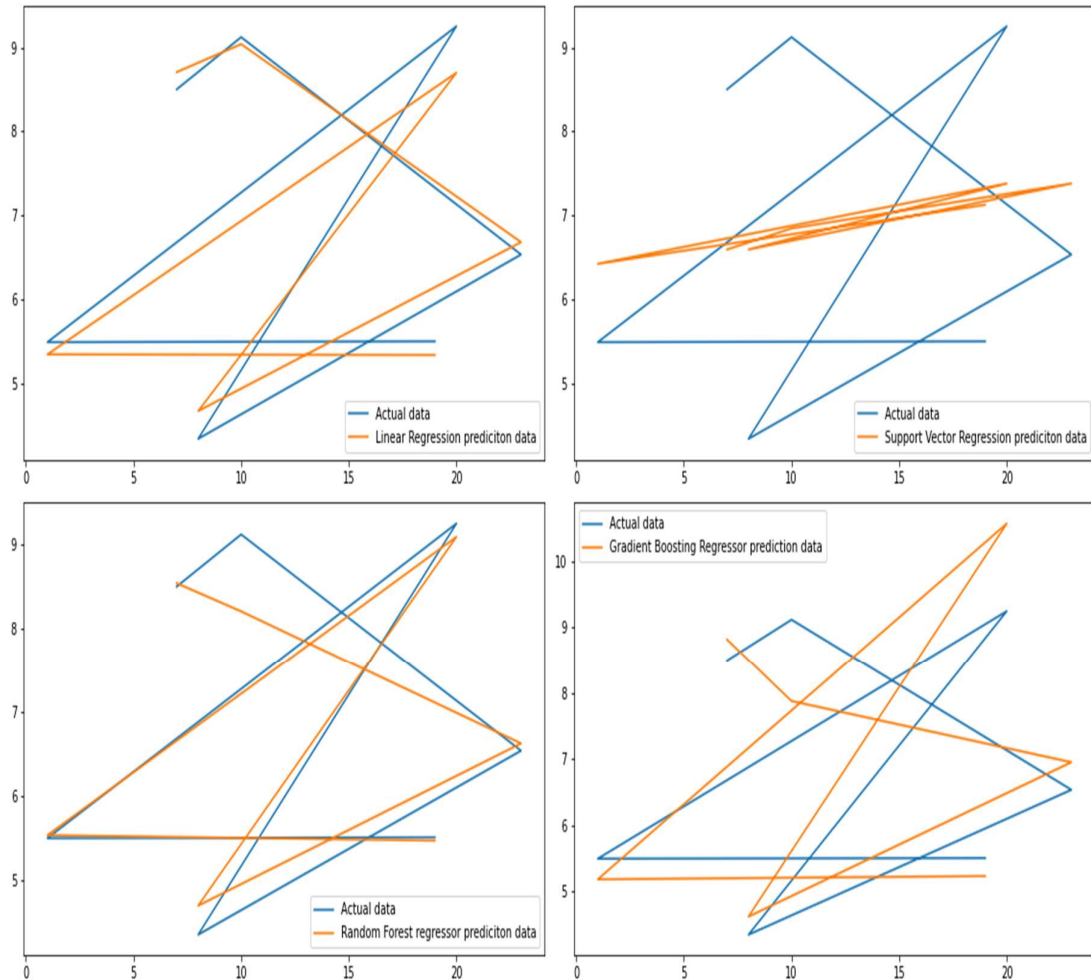
Figure 4.6: Graphical representation of actual data and predicted data of different machine learning algorithm

Random forest regression algorithm gives the prediction result of the experimental data with minimize error, overall all the 4 machine learning algorithm. All the code of the machine learning is written in jupyter notebook and fig. 4.6 is coding generated graphical representation of all machine learning. Table 4.2 shows the actual and predicted results.

Table 4.2: Experimental and predicted value of surface roughness of samples through Random forest repressor model

Experiment No.	Actual SR (Ra)	Predicted SR (Ra)	Absolute % error
1	4.20	4.432	5.523
2	5.61	5.364	4.38
3	6.34	6.3307	0.14
4	7.51	8.006	6.60
5	9.28	8.89	4.20
6	6.62	6.5178	1.54
7	7.86	7.9154	0.70
8	8.45	8.569	1.48
9	4.4	4.738	7.68
10	5.78	5.6902	1.55
11	9.13	8.2075	10.104
12	4.55	5.02	10.329
13	5.84	5.84	0
14	6.70	6.73	0.447
15	8.30	8.11	2.289
16	6.20	6.14	0.96
17	7.31	7.059	3.433
18	8.55	8.29	3.04
19	7.6	8.28	8.947
20	5.43	5.57	2.578
21	9.34	9.123	2.3233
22	10.02	9.446	5.72
23	6.76	6.129	9.33
24	6.6	6.55	0.75
25	8.35	7.79	6.706

4.4. XRD ANALYSIS

X-ray diffraction analysis was used to determine amorphous and crystalline structure with degree of crystallinity. The XRD result of PLA+ polymer material is shown in figure 4.7 .Because PLA is a semi-crystalline polymer, it was expected to generate X-ray diffractometry peaks, [98] PLA+ (Polylactic Acid+ or advanced PLA) is also a semicrystalline polymer . This means that it does contain both crystalline and amorphous regions, its overall structure exhibits a combination of crystallinity and amorphousness. The peak of 2theta is approx. on 18 degree approximate.
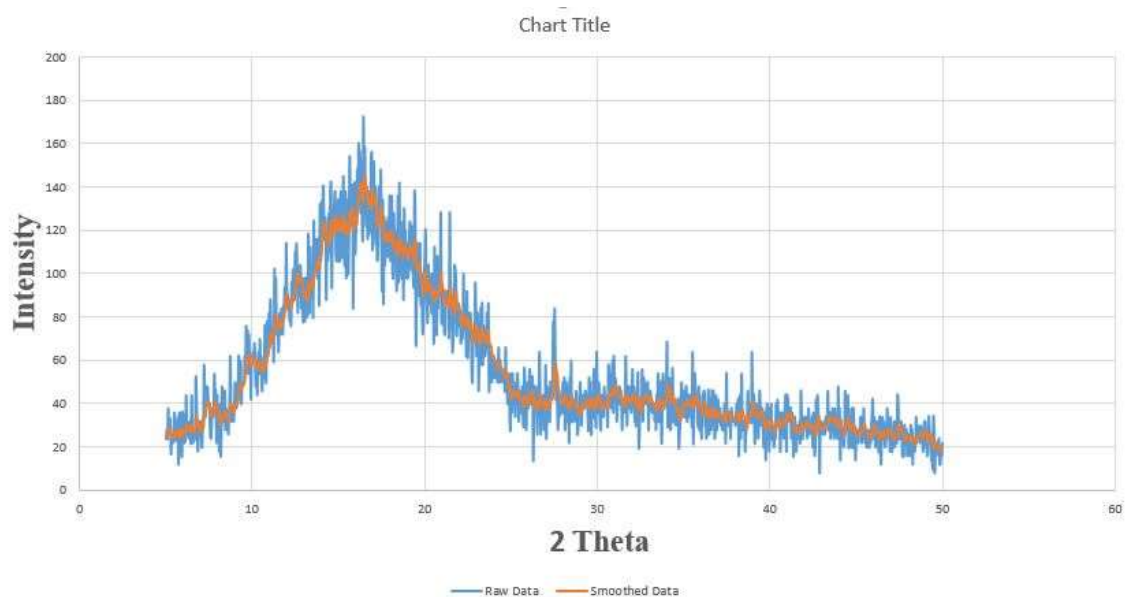
Figure 4.7: XRD results of PLA+ material

In its solid state, PLA forms crystalline regions where the polymer chains are arranged in an ordered and repeating pattern. These crystalline regions contribute to the material's stiffness and strength. However, PLA+ also contains amorphous regions where the polymer chains are randomly oriented, lacking a distinct pattern. The amorphous regions give PLA its transparency and flexibility. Peak positions are expressed in terms of the diffraction angle (2θ), which is related to the spacing between crystallographic planes in the material. The intensity of the peaks is proportional to the amount of scattering occurring from those planes. The shape and width of the peaks can provide insights into factors like crystallite size, strain, and crystal orientation.

The degree of crystallinity in PLA can be influenced by various factors, including the processing conditions during manufacturing and the cooling rate of the material. Generally, PLA has a relatively low crystallinity compared to some other semicrystalline

polymers. It's worth noting that the presence of crystalline and amorphous regions in PLA+ affects its properties. For example, the crystalline regions contribute to its higher melting point and rigidity, while the amorphous regions contribute to its lower glass transition temperature and flexibility.

4.5. Microhardness analysis

Analyze the microhardness experimental data shows that the influence of infill density, printing speed, and nozzle temperature and layer height all parameters play a important role in the microhardness of the PLA+ polymer material which is shown in the figure 4.8. The micro hardness values of the PLA+ material are higher compared to standard PLA, it can be concluded that the addition of additives or modifications have successfully improved the hardness properties of the material. This enhancement may be attributed to factors such as increased filler content, reinforcement materials, or changes in processing parameters.
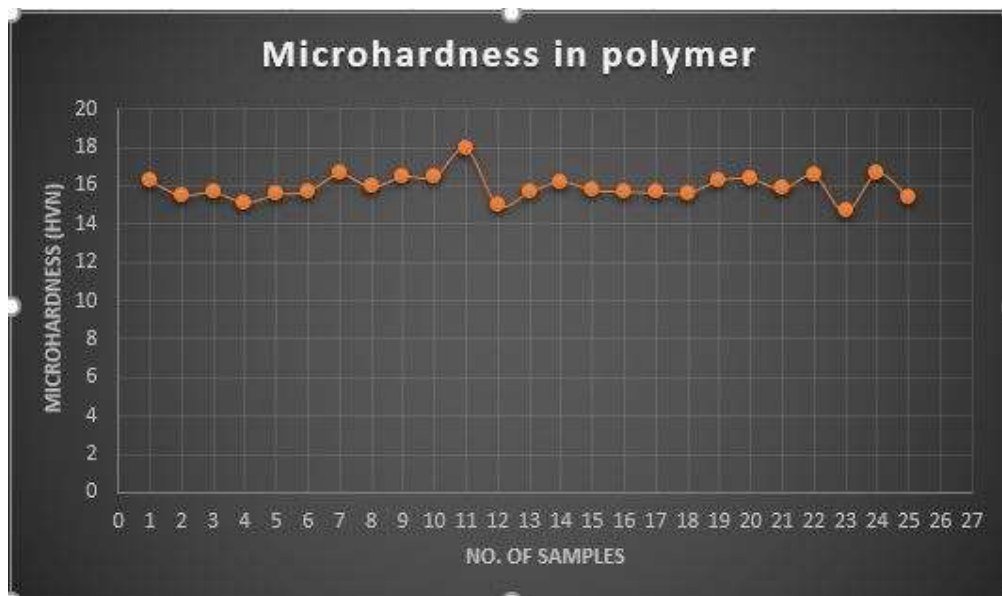

Figure 4.8. Microhardness in all samples

CHAPTER 5

CONCLUSIONS AND FUTURE WORKS

The surface roughness was measured and 3D samples were fabricated successfully using the L25 orthogonal array. The study proposed a data-driven framework that utilized machine learning to predict surface roughness and dimensional accuracy, and obtain optimal process parameters. Verification experiments showed that the optimized results were consistent with experimental results, indicating the effectiveness and feasibility of the proposed method. The study concluded that using machine learning to study process parameters and obtain optimal settings for surface roughness is a viable approach.

1. Surface roughness is directly depend on the parameters of layer height and printing speed, With the increase of layer height, Printing speed, that directly effect to increase the surface roughness of the 3d printing parts. Layer height is 89% positive correlation with the surface roughness and printing speed is 30% correlation with the surface roughness. Surface roughness is minimum gives less wear with the meshing parts

2. Infill density and nozzle temperature gives constant relation between the surface roughness's does not gives any type of effect in the surface roughness. Its approx. 0.030 % correlation with the surface roughness.

3. An ensemble machine learning algorithm random forest repressor is less MSE approx. 0.1255 and maximum r2_Score approx. 0.9685 in all the used machine learning algorithm, with training accuracy is 94.45 and testing accuracy 0.9685 which is also shown in the visualization graph in the figure number 4.6.

4. Increased the metal content in PLA+ polymer may increase the microhardness of the polymer

5. It is a semi crystalline polymer material

Upcoming work involves collecting more data to increase the robustness of the models. Furthermore, new input parameters such as nozzle diameter will be incorporated. Additionally, experimental data will also be utilized in conjunction with or in lieu of numerically generated data to enhance the predictive models. Dynamic measure analysis is also done by the PLA+ material this is my next step work of my research.

Appendices

Appendix 1

linear Regression

```
from sklearn.linear_model import LinearRegression
lr = LinearRegression()
lr.fit(X_train,y_train)
print("Training_Score",lr.score(X_train,y_train))
print("Testing_Score",lr.score(X_test,y_test))

# make predictions on the test set
y_pred = lr.predict(X_test)

# compute the mean squared error
mse = mean_squared_error(y_test, y_pred)
print("mse:", mse)
from sklearn.metrics import r2_score

# Calculate the R2 score between test and predicted data
r2 = r2_score(y_test, y_pred)

# Print the R2 score
print("R2 score:", r2)
# Print the mse
rmse = np.sqrt(mse)
print('rmse:',rmse)
```

Appendix 2

Support vector machine

```python
from sklearn.svm import SVR
svm = SVR()
svm.fit(X_train,y_train)
print("Training_Score",svm.score(X_train,y_train))
print("Testing_Score",svm.score(X_test,y_test))

# make predictions on the test set
y_pred = svm.predict(X_test)

# compute the mean squared error
mse = mean_squared_error(y_test, y_pred)
print("mse:", mse)
from sklearn.metrics import r2_score

# Calculate the R2 score between test and predicted data
r2 = r2_score(y_test, y_pred)

# Print the R2 score
print("R2 score:", r2)

# Print the
rmse = np.sqrt(mse)
print('rmse:',rmse)
```

Appendix 3

Random FOrest Regressor

```python
from sklearn.ensemble import RandomForestRegressor
regressor=RandomForestRegressor(n_estimators=1000, criterion='mse')
regressor.fit(X_train,y_train)
print("Training_Score",regressor.score(X_train,y_train))
print("Training_Score",regressor.score(X_test,y_test))

# make predictions on the test set
y_pred = regressor.predict(X_test)

# compute the mean squared error
mse = mean_squared_error(y_test, y_pred)
print("mse:", mse)
from sklearn.metrics import r2_score

# Calculate the R2 score between test and predicted data
r2 = r2_score(y_test, y_pred)
# Print the R2 score
print("R2 score:", r2)

# Print the mse
rmse = np.sqrt(mse)
print('rmse:',rmse)
```

Appendix 4

Gradient Bossting Regression

```python
from sklearn.ensemble import GradientBoostingRegressor
gr = GradientBoostingRegressor()
gr.fit(X_train,y_train)
print("Training_Score",gr.score(X_train,y_train))
print("Testing_Score",gr.score(X_test,y_test))

# make predictions on the test set
y_pred = gr.predict(X_test)

# compute the mean squared error
mse = mean_squared_error(y_test, y_pred)
print("mse:", mse)
from sklearn.metrics import r2_score

# Calculate the R2 score between test and predicted data
r2 = r2_score(y_test, y_pred)
# Print the R2 score
print("R2 score:", r2)

# Print the mse
rmse = np.sqrt(mse)
print('rmse:',rmse)
```
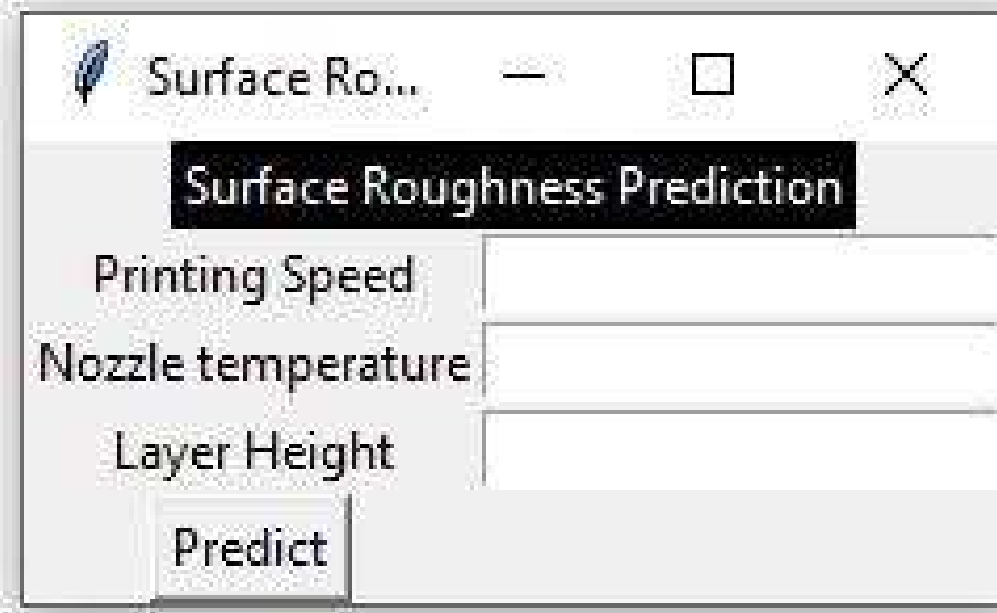
Appendix 5

User interface of surface roughness prediction

REFERENCES

[1] O. A. Mohamed, S. H. Masood, and J. L. Bhowmik, "Optimization of fused deposition modeling process parameters: a review of current research and future prospects," *Adv Manuf*, vol. 3, no. 1, pp. 42–53, Mar. 2015, doi: 10.1007/s40436-014-0097-7.

[2] Y. Zhang *et al.*, "Additive Manufacturing of Metallic Materials: A Review," *Journal of Materials Engineering and Performance*, vol. 27, no. 1. Springer New York LLC, Jan. 01, 2018. doi: 10.1007/s11665-017-2747-y.

[3] S. K. Everton, M. Hirsch, P. I. Stavroulakis, R. K. Leach, and A. T. Clare, "Review of in-situ process monitoring and in-situ metrology for metal additive manufacturing," *Materials and Design*, vol. 95. Elsevier Ltd, pp. 431–445, Apr. 05, 2016. doi: 10.1016/j.matdes.2016.01.099.

[4] R. V. Rao and D. P. Rai, "Optimization of fused deposition modeling process using teaching-learning-based optimization algorithm," *Engineering Science and Technology, an International Journal*, vol. 19, no. 1, pp. 587–603, Mar. 2016, doi: 10.1016/j.jestch.2015.09.008.

[5] Z. Li, Z. Zhang, J. Shi, and D. Wu, "Prediction of surface roughness in extrusion-based additive manufacturing with machine learning," *Robot Comput Integr Manuf*, vol. 57, pp. 488–495, Jun. 2019, doi: 10.1016/j.rcim.2019.01.004.

[6] R. Neelam, S. A. Kulkarni, H. S. Bharath, S. Powar, and M. Doddamani, "Mechanical response of additively manufactured foam: A machine learning approach," *Results in Engineering*, vol. 16, Dec. 2022, doi: 10.1016/j.rineng.2022.100801.

[7] J. Zhang, P. Wang, and R. X. Gao, "Modeling of layer-wise additive manufacturing for part quality prediction," in *Procedia Manufacturing*, Elsevier B.V., 2018, pp. 155–162. doi: 10.1016/j.promfg.2018.10.165.

[8] S. Rouf, A. Raina, M. Irfan Ul Haq, N. Naveed, S. Jeganmohan, and A. Farzana Kichloo, "3D printed parts and mechanical properties: Influencing parameters, sustainability aspects, global market scenario, challenges and applications," *Advanced Industrial and Engineering Polymer Research*, vol. 5, no. 3. KeAi Communications Co., pp. 143–158, Jul. 01, 2022. doi: 10.1016/j.aiepr.2022.02.001.

[9]   D. Horvath, R. Noorani, and M. Mendelson, "Improvement of Surface Roughness on ABS 400 Polymer Using Design of Experiments (DOE)," *Materials Science Forum*, vol. 561–565, pp. 2389–2392, Oct. 2007, doi: 10.4028/www.scientific.net/msf.561-565.2389.

[10]   P. Jiang, M. Rifat, and S. Basu, "Impact of surface roughness and porosity on lattice structures fabricated by additive manufacturing- A computational study," Elsevier B.V., 2020, pp. 781–789. doi: 10.1016/j.promfg.2020.05.114.

[11]   P. Patil, D. Singh, S. J. Raykar, and J. Bhamu, "Multi-objective optimization of process parameters of Fused Deposition Modeling (FDM) for printing Polylactic Acid (PLA) polymer components," in *Materials Today: Proceedings*, Elsevier Ltd, 2021, pp. 4880–4885. doi: 10.1016/j.matpr.2021.01.353.

[12]   S. Dev and R. Srivastava, "Experimental investigation and optimization of FDM process parameters for material and mechanical strength," in *Materials Today: Proceedings*, Elsevier Ltd, 2019, pp. 1995–1999. doi: 10.1016/j.matpr.2020.02.435.

[13]   N. J. Castro and L. G. Zhang, "Biomimetic Nanocomposite Hydrogels for Cartilage Regeneration," in *Nanocomposites for Musculoskeletal Tissue Regeneration*, Elsevier Inc., 2016, pp. 259–281. doi: 10.1016/B978-1-78242-452-9.00012-1.

[14]   X. Bai *et al.*, "Stereolithography additive manufacturing and sintering approaches of SiC ceramics," *Open Ceramics*, vol. 5, Mar. 2021, doi: 10.1016/j.oceram.2020.100046.

[15]   D. Ahn, J. H. Kweon, J. Choi, and S. Lee, "Quantification of surface roughness of parts processed by laminated object manufacturing," *J Mater Process Technol*, vol. 212, no. 2, pp. 339–346, Feb. 2012, doi: 10.1016/j.jmatprotec.2011.08.013.

[16]   H. Agrawaal and J. E. Thompson, "Additive manufacturing (3D printing) for analytical chemistry," *Talanta Open*, vol. 3. Elsevier B.V., Aug. 01, 2021. doi: 10.1016/j.talo.2021.100036.

[17]   M. Pelanconi, P. Colombo, and A. Ortona, "Additive manufacturing of silicon carbide by selective laser sintering of PA12 powders and polymer infiltration and pyrolysis," *J Eur Ceram Soc*, vol. 41, no. 10, pp. 5056–5065, Aug. 2021, doi: 10.1016/j.jeurceramsoc.2021.04.014.

[18]   K. F. Leong, D. Liu, and C. K. Chua, "Tissue Engineering Applications of Additive Manufacturing," in *Comprehensive Materials Processing*, Elsevier Ltd, 2014, pp. 251–264. doi: 10.1016/B978-0-08-096532-1.01010-4.

[19]   D. Oropeza and A. J. Hart, "A laboratory-scale binder jet additive manufacturing testbed for process exploration and material development," *International Journal of Advanced Manufacturing Technology*, vol. 114, no. 11–12, pp. 3459–3473, Jun. 2021, doi: 10.1007/s00170-021-07123-1.

[20]   M. Leary, "Binder jetting," in *Design for Additive Manufacturing*, Elsevier, 2020, pp. 335–339. doi: 10.1016/b978-0-12-816721-2.00013-0.

[21]   O. A. Mohamed, S. H. Masood, and J. L. Bhowmik, "Optimization of fused deposition modeling process parameters: a review of current research and future prospects," *Adv Manuf*, vol. 3, no. 1, pp. 42–53, Mar. 2015, doi: 10.1007/s40436-014-0097-7.

[22]   Y. A. Jin, H. Li, Y. He, and J. Z. Fu, "Quantitative analysis of surface profile in fused deposition modelling," *Addit Manuf*, vol. 8, pp. 142–148, Oct. 2015, doi: 10.1016/j.addma.2015.10.001.

[23]   Z. Liu, Y. Wang, B. Wu, C. Cui, Y. Guo, and C. Yan, "A critical review of fused deposition modeling 3D printing technology in manufacturing polylactic acid parts," *International Journal of Advanced Manufacturing Technology*, vol. 102, no. 9–12. Springer London, pp. 2877–2889, Jun. 19, 2019. doi: 10.1007/s00170-019-03332-x.

[24]   Z. Zhang, Z. Liu, and D. Wu, "Prediction of melt pool temperature in directed energy deposition using machine learning," *Addit Manuf*, vol. 37, Jan. 2021, doi: 10.1016/j.addma.2020.101692.

[25]   X. Li *et al.*, "Qualify assessment for extrusion-based additive manufacturing with 3D scan and machine learning," *J Manuf Process*, vol. 90, pp. 274–285, Mar. 2023, doi: 10.1016/j.jmapro.2023.01.025.

[26]   C. Wang, X. P. Tan, S. B. Tor, and C. S. Lim, "Machine learning in additive manufacturing: State-of-the-art and perspectives," *Additive Manufacturing*, vol. 36. Elsevier B.V., Dec. 01, 2020. doi: 10.1016/j.addma.2020.101538.

[27]   G. D. Goh, S. L. Sing, and W. Y. Yeong, "A review on machine learning in 3D printing: applications, potential, and challenges," *Artif Intell Rev*, vol. 54, no. 1, pp. 63–94, Jan. 2021, doi: 10.1007/s10462-020-09876-9.

[28] R. Li, M. Jin, and V. C. Paquit, "Geometrical defect detection for additive manufacturing with machine learning models," *Mater Des*, vol. 206, Aug. 2021, doi: 10.1016/j.matdes.2021.109726.

[29] M. P. Motta, C. Pelaingre, A. Delamézière, L. Ben Ayed, and C. Barlier, "Machine learning models for surface roughness monitoring in machining operations," in *Procedia CIRP*, Elsevier B.V., 2022, pp. 710–715. doi: 10.1016/j.procir.2022.03.110.

[30] D. Ahn, J. H. Kweon, J. Choi, and S. Lee, "Quantification of surface roughness of parts processed by laminated object manufacturing," *J Mater Process Technol*, vol. 212, no. 2, pp. 339–346, Feb. 2012, doi: 10.1016/j.jmatprotec.2011.08.013.

[31] N. Shahrubudin, T. C. Lee, and R. Ramlan, "An overview on 3D printing technology: Technological, materials, and applications," in *Procedia Manufacturing*, Elsevier B.V., 2019, pp. 1286–1296. doi: 10.1016/j.promfg.2019.06.089.

[32] "3D Printed Turbine in Aluminum PLA." https://www.gcreate.com/post/3d-printed-turbine-in-aluminum-pla (accessed May 29, 2023).

[33] S. C. Joshi and A. A. Sheikh, "3D printing in aerospace and its long-term sustainability," *Virtual Phys Prototyp*, vol. 10, no. 4, pp. 175–185, Oct. 2015, doi: 10.1080/17452759.2015.1111519.

[34] Y. C. Wang, T. Chen, and Y. L. Yeh, "Advanced 3D printing technologies for the aircraft industry: a fuzzy systematic approach for assessing the critical factors," *International Journal of Advanced Manufacturing Technology*, vol. 105, no. 10, pp. 4059–4069, Dec. 2019, doi: 10.1007/s00170-018-1927-8.

[35] "Automotive 3D printing applications." https://www.hubs.com/knowledge-base/automotive-3d-printing-applications/ (accessed May 29, 2023).

[36] V. Sreehitha, "IMPACT OF 3D PRINTING IN AUTOMOTIVE INDUSTRIES," 2017. [Online]. Available: http://iraj.in

[37] M. Petch, "Audi gives update on use of SLM metal 3D printing for the automotive industry," 3D Printing Industry, 2018." https://3dprintingindustry.com/news/audi-gives-update-use-slm-metal-3d-printing-automotive-industry-129376/

[38] R. Bogue, "3D printing: The dawn of a new era in manufacturing?," *Assembly Automation*, vol. 33, no. 4, pp. 307–311, Sep. 2013, doi: 10.1108/AA-06-2013-055.

[39] Y. Liu, Q. Hamid, J. Snyder, C. Wang, and W. Sun, "Evaluating fabrication feasibility and biomedical application potential of in situ 3D printing technology," *Rapid Prototyp J*, vol. 22, no. 6, pp. 947–955, 2016, doi: 10.1108/RPJ-07-2015-0090.

[40] R. Winarso, P. W. Anggoro, R. Ismail, J. Jamari, and A. P. Bayuseno, "Application of fused deposition modeling (FDM) on bone scaffold manufacturing process: A review," *Heliyon*, vol. 8, no. 11. Elsevier Ltd, Nov. 01, 2022. doi: 10.1016/j.heliyon.2022.e11701.

[41] "3D Printed Site Models." https://3dtomorrow.com/2019/10/29/3d-printed-site-models/ (accessed May 29, 2023).

[42] M. Sakin and Y. C. Kiroglu, "3D Printing of Buildings: Construction of the Sustainable Houses of the Future by BIM," in *Energy Procedia*, Elsevier Ltd, 2017, pp. 702–711. doi: 10.1016/j.egypro.2017.09.562.

[43] I. Hager, A. Golonka, and R. Putanowicz, "3D Printing of Buildings and Building Components as the Future of Sustainable Construction?," in *Procedia Engineering*, Elsevier Ltd, 2016, pp. 292–299. doi: 10.1016/j.proeng.2016.07.357.

[44] "Conductive 3D printing offering new opportunities." https://facfox.com/news/transforming-the-electronic-industry-using-3d-printing/ (accessed May 29, 2023).

[45] C. Y. Foo, H. N. Lim, M. A. Mahdi, M. H. Wahid, and N. M. Huang, "Three-Dimensional Printed Electrode and Its Novel Applications in Electronic Devices," *Sci Rep*, vol. 8, no. 1, Dec. 2018, doi: 10.1038/s41598-018-25861-3.

[46] "IannGibsonn· DaviddRosen BrenttStucker Additive Manufacturing Technologies 3D Printing, Rapid Prototyping, and Direct Digital Manufacturing Second Edition."

[47] S. Ford and M. Despeisse, "Additive manufacturing and sustainability: an exploratory study of the advantages and challenges," *J Clean Prod*, vol. 137, pp. 1573–1587, Nov. 2016, doi: 10.1016/j.jclepro.2016.04.150.

[48] Y. Deshpande, A. Andhare, and N. K. Sahu, "Estimation of surface roughness using cutting parameters, force, sound, and vibration in turning of Inconel 718," *Journal of the Brazilian Society of Mechanical Sciences and Engineering*, vol. 39, no. 12, pp. 5087–5096, Dec. 2017, doi: 10.1007/s40430-017-0819-4.

[49] B. N. Turner, R. Strong, and S. A. Gold, "A review of melt extrusion additive manufacturing processes: I. Process design and modeling," *Rapid Prototyping*

Journal, vol. 20, no. 3. Emerald Group Publishing Ltd., pp. 192–204, 2014. doi: 10.1108/RPJ-01-2013-0012.

[50]   F. Lavecchia, M. G. Guerra, and L. M. Galantucci, "Chemical vapor treatment to improve surface finish of 3D printed polylactic acid (PLA) parts realized by fused filament fabrication," *Progress in Additive Manufacturing*, vol. 7, no. 1, pp. 65–75, Feb. 2022, doi: 10.1007/s40964-021-00213-2.

[51]   P. K. Rao, J. Liu, D. Roberson, Z. Kong, and C. Williams, "Online Real-Time Quality Monitoring in Additive Manufacturing Processes Using Heterogeneous Sensors," *Journal of Manufacturing Science and Engineering, Transactions of the ASME*, vol. 137, no. 6, Dec. 2015, doi: 10.1115/1.4029823.

[52]   R. Anitha, S. Arunachalam, and P. Radhakrishnan, "Critical parameters in‾uencing the quality of prototypes in fused deposition modelling."

[53]   M. Domingo-Espin, J. M. Puigoriol-Forcada, A. A. Garcia-Granada, J. Llumà, S. Borros, and G. Reyes, "Mechanical property characterization and simulation of fused deposition modeling Polycarbonate parts," *Mater Des*, vol. 83, pp. 670–677, Oct. 2015, doi: 10.1016/j.matdes.2015.06.074.

[54]   S. Zhang *et al.*, "Novel toughening mechanism for polylactic acid (PLA)/starch blends with layer-like microstructure via pressure-induced flow (PIF) processing," *Mater Lett*, vol. 98, pp. 238–241, 2013, doi: 10.1016/j.matlet.2012.12.019.

[55]   S. Nasiri and M. R. Khosravani, "Machine learning in predicting mechanical behavior of additively manufactured parts," *Journal of Materials Research and Technology*, vol. 14, pp. 1137–1153, Sep. 2021, doi: 10.1016/j.jmrt.2021.07.004.

[56]   A. Boschetto, V. Giordano, and F. Veniali, "3D roughness profile model in fused deposition modelling," *Rapid Prototyp J*, vol. 19, no. 4, pp. 240–252, 2013, doi: 10.1108/13552541311323254.

[57]   A. Boschetto and L. Bottini, "Roughness prediction in coupled operations of fused deposition modeling and barrel finishing," *J Mater Process Technol*, vol. 219, pp. 181–192, 2015, doi: 10.1016/j.jmatprotec.2014.12.021.

[58]   P. Reeves and ac Cobb, "REDUCING THE SURFACE DEVIATION OF STREOLITHOGRAPHY USING AN ALTERNATIVE BUILD STRATERGY."

[59]   D. Ahn, H. Kim, and S. Lee, "Surface roughness prediction using measured data and interpolation in layered manufacturing," *J Mater Process Technol*, vol. 209, no. 2, pp. 664–671, Jan. 2009, doi: 10.1016/j.jmatprotec.2008.02.050.

[60] S. B. Mishra, R. Malik, and S. S. Mahapatra, "Effect of External Perimeter on Flexural Strength of FDM Build Parts," *Arab J Sci Eng*, vol. 42, no. 11, pp. 4587–4595, Nov. 2017, doi: 10.1007/s13369-017-2598-8.

[61] S. B. Mishra, K. Abhishek, M. P. Satapathy, and S. S. Mahapatra, "Parametric Appraisal of Compressive Strength of FDM Build Parts," in *Materials Today: Proceedings*, Elsevier Ltd, 2017, pp. 9456–9460. doi: 10.1016/j.matpr.2017.06.203.

[62] P. M. Pandey, N. V. Reddy, and S. G. Dhande, "Improvement of surface ®nish by staircase machining in fused deposition modeling."

[63] D. Ahn, J. H. Kweon, S. Kwon, J. Song, and S. Lee, "Representation of surface roughness in fused deposition modeling," *J Mater Process Technol*, vol. 209, no. 15–16, pp. 5593–5600, Aug. 2009, doi: 10.1016/j.jmatprotec.2009.05.016.

[64] C. Bellehumeur, L. Li, Q. Sun, and P. Gu, "Modeling of bond formation between polymer filaments in the fused deposition modeling process," *J Manuf Process*, vol. 6, no. 2, pp. 170–178, 2004, doi: 10.1016/S1526-6125(04)70071-7.

[65] A. Garg, A. Bhattacharya, and A. Batish, "On Surface Finish and Dimensional Accuracy of FDM Parts after Cold Vapor Treatment," *Materials and Manufacturing Processes*, vol. 31, no. 4, pp. 522–529, Mar. 2016, doi: 10.1080/10426914.2015.1070425.

[66] C. J. Luis Pérez, "Analysis of the surface roughness and dimensional accuracy capability of fused deposition modelling processes," *Int J Prod Res*, vol. 40, no. 12, pp. 2865–2881, Aug. 2002, doi: 10.1080/00207540210146099.

[67] L. Scime and J. Beuth, "A multi-scale convolutional neural network for autonomous anomaly detection and classification in a laser powder bed fusion additive manufacturing process," *Addit Manuf*, vol. 24, pp. 273–286, Dec. 2018, doi: 10.1016/j.addma.2018.09.034.

[68] M. Harris, J. Potgieter, R. Archer, and K. M. Arif, "Effect of material and process specific factors on the strength of printed parts in fused filament fabrication: A review of recent developments," *Materials*, vol. 12, no. 10. MDPI AG, May 01, 2019. doi: 10.3390/ma12101664.

[69] Y. Zhang and S. K. Moon, "Data-driven design strategy in fused filament fabrication: Status and opportunities," *Journal of Computational Design and Engineering*, vol. 8, no. 2. Oxford University Press, pp. 489–509, Apr. 01, 2021. doi: 10.1093/jcde/qwaa094.

[70] Q. Feng, W. Maier, and H. C. Möhring, "Application of machine learning to optimize process parameters in fused deposition modeling of PEEK material," in *Procedia CIRP*, Elsevier B.V., 2022, pp. 1–8. doi: 10.1016/j.procir.2022.04.001.

[71] N. Ahmed, I. Barsoum, G. Haidemenopoulos, and R. K. A. Al-Rub, "Process parameter selection and optimization of laser powder bed fusion for 316L stainless steel: A review," *Journal of Manufacturing Processes*, vol. 75. Elsevier Ltd, pp. 415–434, Mar. 01, 2022. doi: 10.1016/j.jmapro.2021.12.064.

[72] A. K. Sood, R. K. Ohdar, and S. S. Mahapatra, "Experimental investigation and empirical modelling of FDM process for compressive strength improvement," *J Adv Res*, vol. 3, no. 1, pp. 81–90, Jan. 2012, doi: 10.1016/j.jare.2011.05.001.

[73] H. Bao, S. Wu, Z. Wu, G. Kang, X. Peng, and P. J. Withers, "A machine-learning fatigue life prediction approach of additively manufactured metals," *Eng Fract Mech*, vol. 242, Feb. 2021, doi: 10.1016/j.engfracmech.2020.107508.

[74] R. Kumar, R. Ghosh, R. Malik, K. S. Sangwan, and C. Herrmann, "Development of Machine Learning Algorithm for Characterization and Estimation of Energy Consumption of Various Stages during 3D Printing," in *Procedia CIRP*, Elsevier B.V., 2022, pp. 65–70. doi: 10.1016/j.procir.2022.04.011.

[75] R. V. Pazhamannil, P. Govindan, and P. Sooraj, "Prediction of the tensile strength of polylactic acid fused deposition models using artificial neural network technique," in *Materials Today: Proceedings*, Elsevier Ltd, 2019, pp. 9187–9193. doi: 10.1016/j.matpr.2020.01.199.

[76] A. Pulipaka, K. M. Gide, A. Beheshti, and Z. S. Bagheri, "Effect of 3D printing process parameters on surface and mechanical properties of FFF-printed PEEK," *J Manuf Process*, vol. 85, pp. 368–386, Jan. 2023, doi: 10.1016/j.jmapro.2022.11.057.

[77] A. Maurel *et al.*, "Highly Loaded Graphite-Polylactic Acid Composite-Based Filaments for Lithium-Ion Battery Three-Dimensional Printing," *Chemistry of Materials*, vol. 30, no. 21, pp. 7484–7493, Nov. 2018, doi: 10.1021/acs.chemmater.8b02062.

[78] N. D. Ahmad, Kusmono, M. W. Wildan, and Herianto, "Preparation and properties of cellulose nanocrystals-reinforced Poly (lactic acid) composite filaments for 3D printing applications," *Results in Engineering*, vol. 17, Mar. 2023, doi: 10.1016/j.rineng.2022.100842.

[79] H. El Marouazi *et al.*, "Great enhancement of mechanical features in PLA based composites containing aligned few layer graphene (FLG), the effect of FLG loading, size and dispersion on mechanical and thermal properties."

[80] E. M. Agaliotis *et al.*, "Tensile Behavior of 3D Printed Polylactic Acid (PLA) Based Composites Reinforced with Natural Fiber," *Polymers (Basel)*, vol. 14, no. 19, Oct. 2022, doi: 10.3390/polym14193976.

[81] R. A. Ilyas *et al.*, "Natural Fiber-Reinforced Polylactic Acid, Polylactic Acid Blends and Their Composites for Advanced Applications," *Polymers*, vol. 14, no. 1. MDPI, Jan. 01, 2022. doi: 10.3390/polym14010202.

[82] H. El Marouazi *et al.*, "Great enhancement of mechanical features in PLA based composites containing aligned few layer graphene (FLG), the effect of FLG loading, size and dispersion on mechanical and thermal properties."

[83] M. S. Alsoufi and A. E. Elsayed, "Surface Roughness Quality and Dimensional Accuracy—A Comprehensive Analysis of 100% Infill Printed Parts Fabricated by a Personal/Desktop Cost-Effective FDM 3D Printer," *Materials Sciences and Applications*, vol. 09, no. 01, pp. 11–40, 2018, doi: 10.4236/msa.2018.91002.

[84] S. Ravinder, & Chintireddy, and S. Reddy, "OPTIMIZATION OF 3D PRINTING PARAMETERS ON SURFACE ROUGHNESS BY TAGUCHI METHOD." [Online]. Available: www.tjprc.org

[85] M. Sumalatha, J. N. Malleswara Rao, and B. Supraja Reddy, "Optimization Of Process Parameters In 3d Printing-Fused Deposition Modeling Using Taguchi Method," *IOP Conf Ser Mater Sci Eng*, vol. 1112, no. 1, p. 012009, Apr. 2021, doi: 10.1088/1757-899x/1112/1/012009.

[86] A. Cano-Vicent *et al.*, "Fused deposition modelling: Current status, methodology, applications and future prospects," *Additive Manufacturing*, vol. 47. Elsevier B.V., Nov. 01, 2021. doi: 10.1016/j.addma.2021.102378.

[87] Rasyidah, R. Efendi, N. M. Nawi, M. M. Deris, and S. M. A. Burney, "Cleansing of inconsistent sample in linear regression model based on rough sets theory," *Systems and Soft Computing*, vol. 5, Dec. 2023, doi: 10.1016/j.sasc.2022.200046.

[88] "Linear Regression in Machine Learning." https://www.javatpoint.com/linear-regression-in-machine-learning (accessed May 29, 2023).

[89] M. Ulas, O. Aydur, T. Gurgenc, and C. Ozel, "Surface roughness prediction of machined aluminum alloy with wire electrical discharge machining by different

machine learning algorithms," *Journal of Materials Research and Technology*, vol. 9, no. 6, pp. 12512–12524, Nov. 2020, doi: 10.1016/j.jmrt.2020.08.098.

[90]   "Support Vector Machine: Regression." https://www.fromthegenesis.com/support-vector-machine-regression/ (accessed May 29, 2023).

[91]   "Random Forest Algorithms." https://www.analyticsvidhya.com/blog/2021/06/understanding-random-forest/ (accessed May 29, 2023).

[92]   N. Hooda, J. S. Chohan, R. Gupta, and R. Kumar, "Deposition angle prediction of Fused Deposition Modeling process using ensemble machine learning," *ISA Trans*, vol. 116, pp. 121–128, Oct. 2021, doi: 10.1016/j.isatra.2021.01.035.

[93]   "Boosting Algorithms." https://towardsdatascience.com/boosting-algorithms-explained-d38f56ef3f30 (accessed May 29, 2023).

[94]   R. Cai, K. Wang, W. Wen, Y. Peng, M. Baniassadi, and S. Ahzi, "Application of machine learning methods on dynamic strength analysis for additive manufactured polypropylene-based composites," *Polym Test*, vol. 110, Jun. 2022, doi: 10.1016/j.polymertesting.2022.107580.

[95]   M. Cheng *et al.*, "Prediction and evaluation of surface roughness with hybrid kernel extreme learning machine and monitored tool wear," *J Manuf Process*, vol. 84, pp. 1541–1556, Dec. 2022, doi: 10.1016/j.jmapro.2022.10.072.

[96]   W. Alhaddad, M. He, Y. Halabi, and K. Yahya Mohammed Almajhali, "Optimizing the material and printing parameters of the additively manufactured fiber-reinforced polymer composites using an artificial neural network model and artificial bee colony algorithm," *Structures*, vol. 46, pp. 1781–1795, Dec. 2022, doi: 10.1016/j.istruc.2022.10.134.

[97]   T. M. Díez-Rodríguez, E. Blázquez-Blázquez, E. Pérez, and M. L. Cerrada, "Composites based on poly(Lactic acid) (pla) and sba-15: Effect of mesoporous silica on thermal stability and on isothermal crystallization from either glass or molten state," *Polymers (Basel)*, vol. 12, no. 11, pp. 1–22, Nov. 2020, doi: 10.3390/polym12112743.

[98]   F. A. dos Santos, G. C. V. Iulianelli, and M. I. B. Tavares, "Effect of microcrystalline and nanocrystals cellulose fillers in materials based on PLA matrix," *Polym Test*, vol. 61, pp. 280–288, Aug. 2017, doi: 10.1016/j.polymertesting.2017.05.028.

LIST OF PUBLICATION

Scopus Preview

Sources

Title ⌄ | Enter title | **Find sources**

Title: European Chemical Bulletin ✕

Filter refine list

Apply   Clear filters

Display options ⌃

☐ Display only Open Access journals

Counts for 4-year timeframe

○ No minimum selected

○ Minimum citations

○ Minimum documents

Citescore highest quartile

☐ Show only titles in top 10 percent

☐ 1st quartile

☐ 2nd quartile

☐ 3rd quartile

☐ 4th quartile

Source type ⌃

☐ Journals

☐ Book Series

☐ Conference Proceedings

☐ Trade Publications

Apply   Clear filters

1 result

⬇ Download Scopus Source List   ⓘ Learn more about Scopus Source List

☐ All ⌄   ⬛ Export to Excel   💾 Save to source list

View metrics for year: 2022 ⌄

☐	Source title ↓	CiteScore ↓	Highest percentile ↓	Citations 2019-22 ↓	Documents 2019-22 ↓	% Cited ↓	❯
☐ 1	European Chemical Bulletin *Open Access*	1.6	33% 273/407 General Chemistry	509	313	39	

⌃ Top of page

About Scopus

What is Scopus

Content coverage

Scopus blog

Scopus API

Privacy matters

Language

日本語版を表示する

查看简体中文版本

查看繁體中文版本

Просмотр версии на русском языке

Customer Service

Help

Tutorials

Contact us